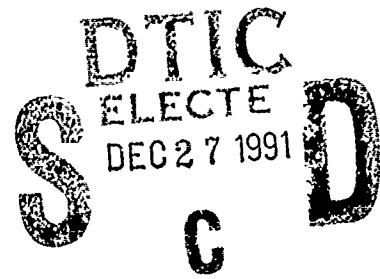


AD-A243 696



AFIT/GE/ENG/91D-46



Sensing Refractive Turbulence Profiles
Using Wave Front Slope Measurements
From Two Reference Sources

THESIS

Michael David Rejack
Captain, USAF

AFIT/GE/ENG/91D-46

91-18987



Approved for public release; distribution unlimited

91 12 24 031

REPORT DOCUMENTATION PAGE			Form Approved OMB No. 0704-0188	
<small>Public reporting burden for this collection of information is estimated to average 1 hour per response, including the time for reviewing instructions, searching existing data sources, gathering and maintaining the data needed, and completing and reviewing this collection of information. Send comments regarding this burden estimate or any other aspect of this collection of information, including suggestions for reducing this burden, to Washington Headquarters Services, Directorate for Information Operations and Reports, 1215 Jefferson Davis Highway, Suite 1204, Arlington, VA 22202-4302, and to the Office of Management and Budget, Paperwork Reduction Project (0704-0188), Washington, DC 20503.</small>				
1. AGENCY USE ONLY (Leave blank)	2. REPORT DATE December 1991	3. REPORT TYPE AND DATES COVERED Master's Thesis		
4. TITLE AND SUBTITLE Sensing Refractive Turbulence Profiles Using Wave Front Slope Measurements From Two Reference Sources			5. FUNDING NUMBERS	
6. AUTHOR(S) Michael D. Rejack, Captain, USAF				
7. PERFORMING ORGANIZATION NAME(S) AND ADDRESS(ES) Air Force Institute of Technology WPAFB, OH 45433-6583			8. PERFORMING ORGANIZATION REPORT NUMBER AFIT/GE/ENG/91D-46	
9. SPONSORING / MONITORING AGENCY NAME(S) AND ADDRESS(ES) Captain Michael Roggemann Phillips Lab/ARCI Kirtland AFB, N.M. 87117			10. SPONSORING / MONITORING AGENCY REPORT NUMBER	
11. SUPPLEMENTARY NOTES				
12a. DISTRIBUTION / AVAILABILITY STATEMENT Approved for Public Release; Distribution Unlimited			12b. DISTRIBUTION CODE	
13. ABSTRACT (Maximum 200 words) This thesis examines a remote sensing technique for measuring the atmospheric structure constant as a function of altitude by performing spatial correlation of wave front sensor measurements. Two point sources are used to irradiate two wave front sensors in the aperture plane of an optical system. The geometric relationship between the sources and the sensors gives rise to crossed optical paths. At the point where the paths cross, the correlation value of the turbulence contributions will be at a peak. The correlation is shown to be mathematically related to the structure constant in terms of an integral of the structure constant multiplied by a path weighting function. It is shown that the path weighting function can be made to have the characteristics of a sampling function and the value of the structure constant can be directly inferred from the correlation measurement. The vertical resolution and signal-to-noise ratio are calculated for a sample case of two-layer turbulence.				
14. SUBJECT TERMS Atmospheric Refraction, Refractive Index, Atmospheric Motion, Atmospheric Turbulence, Structure Constant, Remote Sensing			15. NUMBER OF PAGES 68	
			16. PRICE CODE	
17. SECURITY CLASSIFICATION OF REPORT Unclassified	18. SECURITY CLASSIFICATION OF THIS PAGE Unclassified	19. SECURITY CLASSIFICATION OF ABSTRACT Unclassified	20. LIMITATION OF ABSTRACT UL	

AFIT/GE/ENG/91D-46

Sensing Refractive Turbulence Profiles Using Wave Front Slope Measurements
From Two Reference Sources

THESIS

Presented to the Faculty of the School of Engineering
of the Air Force Institute of Technology
Air University
In Partial Fulfillment of the
Requirements for the Degree of
Master of Science in Electrical Engineering

Michael David Rejack, B.S.
Captain, USAF

December 1991

Accession For	
NTIS GRA&I	<input checked="checked" type="checkbox"/>
DTIC TAB	<input type="checkbox"/>
Unannounced	<input type="checkbox"/>
Justification	
By _____	
Distribution/	
Availability Codes	
Dist	Avail and/or Special
A-1	



Approved for public release; distribution unlimited

Acknowledgments

I would like to thank my thesis advisor, Captain Byron M. Welsh, for his assistance with this research project. I would also like to thank my children, Nicholas and Emily, for leaving behind friends and a home they loved in Colorado to follow me to another unknown place. They are the two best kids a dad could ever wish for. I would especially like to thank my wife, Cheryl, who, through it all, is still the best friend I have ever had.

Michael David Rejack

Table of Contents

	Page
Acknowledgments	ii
Table of Contents	iii
List of Figures	vi
Abstract	vii
 I. Introduction	 1-1
1.1 Atmospheric Turbulence	1-1
1.2 Characterization of Turbulence	1-2
1.3 Measurement of C_n^2	1-2
1.4 Approach	1-2
1.5 Overview	1-3
 II. Background	 2-1
2.1 Introduction	2-1
2.2 Theory	2-1
2.2.1 Atmospheric Turbulence	2-1
2.2.2 Power Spectral Density	2-1
2.2.3 Kolmogoroff Spectrum	2-2
2.3 Evaluation of C_n^2	2-2
2.3.1 Correlation of Irradiance Measurements	2-3
2.3.2 The Crossed-Beam Method	2-3
2.4 Conclusion	2-4

	Page
III. Methodology	3-1
3.1 Introduction	3-1
3.2 Overview of Derivation	3-3
3.3 Derivation of the Path Weighting Function	3-3
3.3.1 Correlation of Slope Signals	3-3
3.3.2 Ensemble Average of C_s	3-5
3.3.3 Path Weighting Function	3-7
3.3.4 Evaluation of Path Weighting Function	3-8
3.3.5 Simplification of Path Weighting Function	3-10
3.4 Improvement of the Path Weighting Function	3-13
3.5 Signal-to-Noise Ratio of the Correlation Measurement	3-13
3.5.1 Derivation of the Variance	3-14
3.5.2 Reduction of the Variance Expression	3-19
3.5.3 SNR Equation	3-20
3.6 Conclusion	3-21
IV. Findings and Results	4-1
4.1 Introduction	4-1
4.2 Characteristics of the Path Weighting Function	4-1
4.2.1 Unmodified Path Weighting Function	4-2
4.2.2 Modified Path Weighting Function	4-3
4.3 Resolution of the Path Weighting Function	4-4
4.4 Signal-to-Noise Ratio of the Correlation Measurement	4-7
4.4.1 SNR as a Function of Noise	4-8
4.4.2 SNR as a Function of Ray Path Separation	4-9
4.4.3 Improvement of the SNR	4-11
4.5 Obtaining a Vertical Profile	4-11
4.6 Conclusion	4-12

	Page
V. Conclusions and Recommendations	5-1
5.1 Overview	5-1
5.2 Conclusions	5-1
5.3 Recommendations	5-1
5.4 Summary	5-2
Appendix A. Computer Programs	A-1
A.1 Program NORMPATH	A-1
A.2 Program MODPWF	A-3
A.3 Program SNR	A-6
Bibliography	BIB-1
Vita	VITA-1

List of Figures

Figure	Page
1.1. Measurement Geometry	1-3
2.1. C_n^2 As A Function Of Altitude	2-2
3.1. Measurement Geometry	3-1
4.1. Normalized Path Weighting Function	4-2
4.2. Modified Path Weighting Function	4-3
4.3. Vertical Resolution	4-6
4.4. SNR as a Function of Photon Count	4-8
4.5. SNR as a Function of Subaperture Separation	4-10
4.6. SNR as a Function of Source Separation	4-10

Abstract

This thesis examines a remote sensing technique for measuring the atmospheric structure constant (C_n^2) as a function of altitude by performing spatial correlation of wave front sensor measurements. Two point sources are used to irradiate two wave front sensors in the aperture plane of an optical system. The geometric relationship between the sources and the sensors gives rise to crossed optical paths. At the point where the paths cross, the correlation value of the turbulence contributions will be at a peak. The correlation is shown to be mathematically related to the structure constant in terms of an integral of C_n^2 multiplied by a path weighting function. It is shown that the path weighting function can be made to have the characteristics of a sampling function and the value of the structure constant can be directly inferred from the correlation measurement. The vertical resolution and signal-to-noise ratio are calculated for a sample case of two-layer turbulence.

Sensing Refractive Turbulence Profiles Using Wave Front Slope Measurements From Two Reference Sources

I. Introduction

1.1 Atmospheric Turbulence

An electromagnetic wave traveling through the Earth's atmosphere is subject to a phenomena known as atmospheric turbulence. Atmospheric turbulence, caused by differential heating of the Earth's surface by the sun, is characterized by random variations in atmospheric temperature and pressure. An electromagnetic wave passing through turbulence experiences a bending or distortion of the wave front shape. Optical systems operating in the presence of the atmosphere are subject to the effects of the turbulence. The distortion reduces the resolution the astronomer achieves when looking through a telescope and disrupts optical communications. The familiar twinkling of starlight is an example of the distortion caused by the atmosphere. The light waves are being bent as they pass through the atmosphere to the Earth.

The efforts to mitigate the effect of atmospheric turbulence on optical systems spawned a branch of optics known as adaptive optics. In adaptive optics, techniques are employed to reverse the effects of the atmosphere on the optical wave (7). One common technique is to use a deformable mirror. A control system senses the deformation of the incoming wave front and sends signals to the mirror. The mirror surface deforms to a shape that is the inverse of the distortion. When the distorted wave hits the deformed mirror, the distortion is nullified.

Inherent in the techniques of adaptive optics is the need to be able to characterize the nature of the wave front distortion. To characterize the wave front distortion, it is necessary to know how the turbulence is distributed along the optical path. A parameter known as the atmospheric structure constant is commonly used as a measure of the strength of the turbulence. The structure constant is introduced in the following section.

1.2 Characterization of Turbulence

The atmosphere may be thought of as a random field. The pressure and temperature change as a function of position. Therefore, the pressure and temperature are non-uniformly distributed along an optical propagation path. In the theory of turbulence, the strength of the turbulence is characterized by the magnitude of the power spectral density (psd) of the index of refraction, n . This psd is designated as $\Phi_n(\vec{k})$ where \vec{k} is the wavenumber vector.

The magnitude of $\Phi_n(\vec{k})$ is proportional to a parameter known as the atmospheric structure constant of the refractive index fluctuations. The atmospheric structure constant is denoted as C_n^2 and is a function of position along the optical path. Since the magnitude of the psd is proportional to C_n^2 , C_n^2 is used as a measure of the strength of the turbulence.

1.3 Measurement of C_n^2

There have been numerous methods used to measure C_n^2 (3, 10, 12, 14, 17). Actually, the use of the word measurement is a misnomer since the structure constant can not be directly measured with any kind of instrument. The technique used to evaluate C_n^2 is to measure a parameter of an optical system operating in the presence of turbulence and extract the value of C_n^2 from the measured quantity. Fried (3) was one of the first to apply this approach by performing a spatial cross-correlation of stellar scintillation measurements. As with Fried's work, current techniques rely primarily on the spatial or temporal cross correlation properties of the intensity of the optical field. This research will take a new approach, based not on the intensity of the optical field, but on the correlation properties of the wave front phase.

1.4 Approach

Consider two point sources, denoted p_1 and p_2 , which are separated by a distance Δp as shown in figure 1.1. Two wave front sensors are placed in the aperture plane of the optical system. The geometric relationship between the sources and the wave front sensors gives rise to crossed optical paths. The light from each point source travels a different optical path to the wave front sensors. At the point where the paths cross, the turbulence contributions from the two sources will be highly correlated. This correlation is exploited to calculate C_n^2 . A three step process is used in this thesis. It is first shown that the structure constant is related to the correlation of the measurements from the two wave

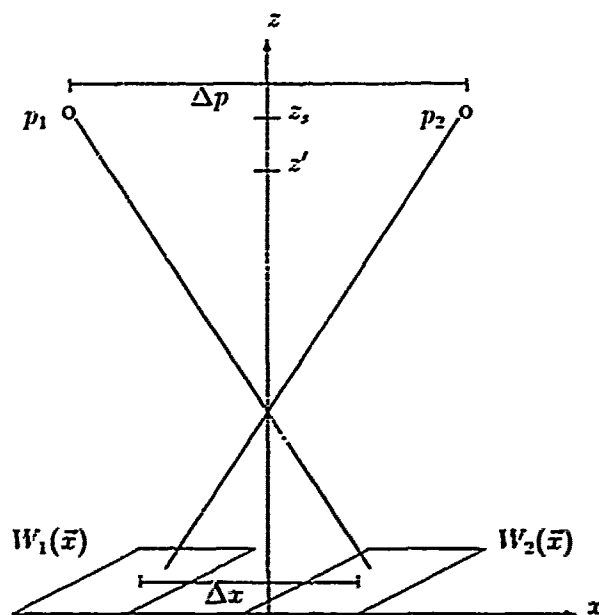


Figure 1.1. Measurement Geometry

front sensors by

$$C_s = \int dz C_n^2(z') w(z') \quad (1.1)$$

where C_s is the correlation of wave front sensor measurement 1 with wave front sensor measurement 2, z' is a position along the vertical path, and $w(z')$ is a path weighting function. The next step proves that the weighting function can be shown to approximate a Dirac delta function under certain conditions. The sifting property of the Dirac delta function may be used to evaluate C_n^2 from the relationship in equation 1.1. Finally, the signal-to-noise ratio (SNR) of the correlation measurement is calculated to evaluate the accuracy of the method.

1.5 Overview

Chapter II reviews the background of atmospheric turbulence sensing as it applies to this research. Chapter III explains the methodology employed in this research. Chapter IV is a presentation and analysis of the results. Chapter V contains conclusions and recommendations for further study.

II. Background

2.1 Introduction

This chapter examines the theory of atmospheric turbulence and reviews a method used by Fried to calculate the strength of the turbulence. The crossed-beam method of remote sensing, and its' application to this research, is discussed.

2.2 Theory

2.2.1 Atmospheric Turbulence The index of refraction, n , for a medium is the ratio of the speed of light in a vacuum to that in the medium. In the Earth's atmosphere, n is a function of pressure, temperature, and humidity. As such, it varies with height above the Earth's surface and n may be expressed as a function of position. The variation of the index of refraction is a random quantity. The atmosphere may be visualized as consisting of randomly sized pockets of air called eddies. Typically, eddies range in size from a few millimeters to tens of meters. Each eddie is at a different pressure and temperature and thus has a different n . As an optical wave front propagates through the atmosphere, the variation in n from eddie to eddie distorts the wave front.

Since the characteristics of the eddies are random, n is a temporal and spatial random process. As a result, it is necessary to use statistical methods to describe the characteristics of n . In atmospheric optics, it is common to characterize the second order statistics of n using the structure function. Using angle brackets to denote the ensemble average, the structure function is given by (8:526-527)

$$D_n(\vec{r}) = \langle |n(\vec{r} + \vec{r}_1) - n(\vec{r}_1)|^2 \rangle \quad (2.1)$$

where \vec{r} is a position vector.

2.2.2 Power Spectral Density The power spectral density (psd) of the index of refraction fluctuations, $\Phi_n(\vec{K})$, is a measure of the strength of the turbulence. As Goodman states, (6:388) the psd may be regarded as a measure of the relative occurrence of eddies with dimensions $L = \frac{2\pi}{|\vec{K}|}$. \vec{K} is called the wavenumber vector and may be interpreted as the number of eddies that occur in a unit length. As Tatarski shows (15:19-21), the psd may be related to the structure function by

$$D_n(\vec{r}) = 2 \int \int_{-\infty}^{\infty} [1 - \cos(\vec{K} \cdot \vec{r})] \Phi_n(\vec{K}) d^3 \vec{K} \quad (2.2)$$

2.2.3 Kolmogoroff Spectrum In a classic paper on statistical theory (9), Kolmogoroff developed a theory of turbulence that has been used to model the effects of the atmosphere. In this theory, the eddies are characterized by two size parameters; the outer scale L_o and the inner scale l_o . If the eddie size is between L_o and l_o (i.e. $\frac{2\pi}{L_o} < K < \frac{2\pi}{l_o}$), the turbulence is essentially isotropic and this region is known as the inertial subrange. Since the turbulence is isotropic, Φ_n is only a function of the magnitude of \vec{K} and the spectrum is expressed as (6:386-390)

$$\Phi_n(K) = 0.033 C_n^2 K^{-\frac{11}{3}} \quad (2.3)$$

where $K = |\vec{K}|$. The quantity C_n^2 is known as the structure constant of the refractive index fluctuations and is used as a measure of the strength of the turbulence.

2.3 Evaluation of C_n^2

It is not possible to measure C_n^2 directly, however, the evaluation of C_n^2 as a function of position has been widely studied. Both vertical and horizontal profiles have been obtained, however, the vertical profile is of primary interest for celestial imaging. Figure 2.1, adapted from tabular data in reference (1:2179), is a plot of a typical vertical profile of C_n^2 from 1 to 20 kilometers.

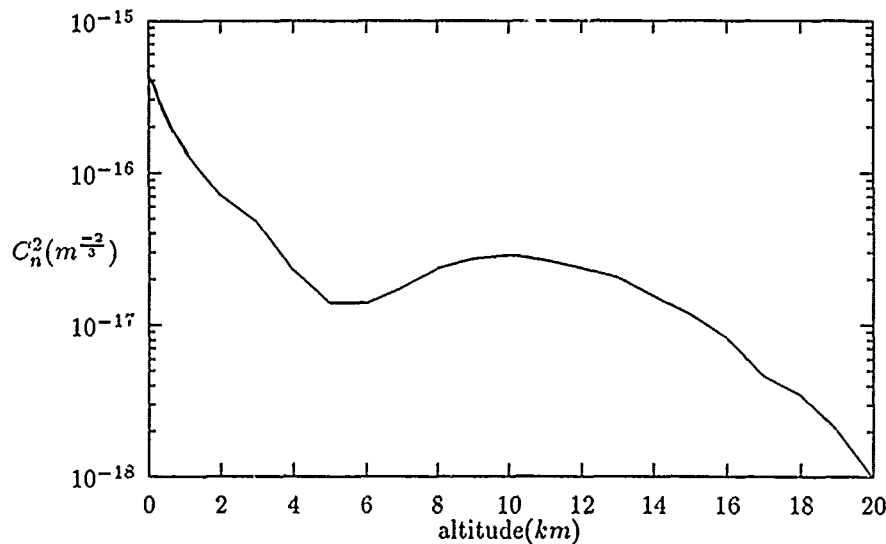


Figure 2.1. C_n^2 As A Function Of Altitude

In 1968, Peskoff (13) published a mathematical basis for calculating C_n^2 . He proposed gathering irradiance data from optical scintillations and correlating the irradiance measurements. The correlation value is used to extract C_n^2 . At the same time, Fried proposed a similar experimental implementation (3). Fried's work is a good example of the correlation method and is explained in the following section.

2.3.1 Correlation of Irradiance Measurements Fried proposed using two telescopes, each having a restricted field of view, to track scintillating stars and gather irradiance data (3:416-418). The intensities measured by the telescopes are denoted $i_1(t)$ and $i_2(t)$ where t is time. The logarithmic amplitude, $l_i(t)$, is computed from the relationship

$$l_i(t) = \frac{1}{2} \ln \left[\frac{i_i(t)}{\langle i_i(t) \rangle} \right] \quad (2.4)$$

where the angle brackets denote a time average. In turn, the spatial-temporal log amplitude covariance $C_l(\rho, \tau)$ is calculated from the log-amplitudes by

$$C_l(\rho, \tau) = \langle [l_1(t) - \langle l_1(t) \rangle] [l_2(t + \tau) - \langle l_2(t) \rangle] \rangle \quad (2.5)$$

Tatarski's work (15:110-113) contains an equation which relates $C_l(\rho, \tau)$ to C_n^2 . Fried applies this equation and reduces the resultant integral to the following form:

$$C_l(\rho) = k^{\frac{5}{6}} \int_0^\infty dz z^{\frac{5}{6}} C_n^2(z) F\left(\frac{kp^2}{4z}\right) \quad (2.6)$$

In this expression, $F\left(\frac{kp^2}{4z}\right)$ is a function that represents a grouping of all the mathematical terms that depend on $\frac{kp^2}{4z}$. This allows C_n^2 and z to stand alone in the integral. Fried analytically solves the function $F\left(\frac{kp^2}{4z}\right)$ and provides a table of values. Using this table, the measured $C_l(\rho)$ is now related to the unknown $C_n^2(z)$ by a linear integral equation.

The approach used by Fried has become somewhat standard. Measurements are made of a property of an optical field and the measured quantities are related to C_n^2 (usually by an integral). The terms in the equation are grouped into a separate function to allow C_n^2 to stand alone. The separate function is called a path weighting function and relates C_n^2 to the measured quantity.

2.3.2 The Crossed-Beam Method In 1967, Fisher and Krause (2) proposed a method to extract turbulence values from measurements made using crossed laser beams. Two laser

beams intersect at a right angle in a turbulent medium. At the point of intersection, there is a related (correlated) fluctuation in both beams. Away from the intersection point, the turbulence effects are uncorrelated and produce uncorrelated effects on the beams. If the covariance is calculated, the uncorrelated effects yield a zero average value while the correlated effects yield a non-zero average value. The correlation value at the intersection is a function of the magnitude of the turbulence fluctuations at or near the intersection point. The covariance values can be used to evaluate the strength of the turbulence. They show the method produces accurate results for measuring turbulence in the shear layer of a subsonic jet.

In 1974, Wang and his colleagues (17) applied the crossed beam theory to sense horizontal wind and refractive turbulence profiles. They did not require the beams to be perpendicular. Calculating the covariance function of intensity fluctuations of the crossed-path signals, their development yields an expression very similar to equation 1.1. C_n^2 is related to the covariance by an integral involving a weighting function. They profile the weighting functions for three different transmitter-receiver configurations.

2.4 Conclusion

Characterizing the strength of atmospheric turbulence by remote sensing has been widely studied. The crossed-beam method is often used to measure a parameter of an optical field. The measured values are related to the atmospheric structure constant, and the structure constant serves as a measure of the strength of the turbulence. Much of the past work has concentrated on optical scintillation measurements where the intensity of the light is the quantity of interest. It is proposed that crossed beams may be used to obtain a measurement of wave front phase, rather than intensity, and the phase correlation properties may be used to calculate C_n^2 . The next chapter presents the development of this proposal.

III. Methodology

3.1 Introduction

As discussed in the previous chapter, a primary method used to obtain vertical profiles of C_n^2 has been through the use of optical scintillation measurements. These measurements utilize the intensity of the optical field. Instead of using intensity as the quantity of interest, it is shown in this chapter that measurements of wave front phase slope may be used to obtain profiles of C_n^2 .

Consider two point sources, located at points p_1 and p_2 , and separated by a vector distance $\Delta \vec{p}$, as shown in figure 3.1. Two wave front sensors, $W_1(\vec{x})$ and $W_2(\vec{x})$, are placed

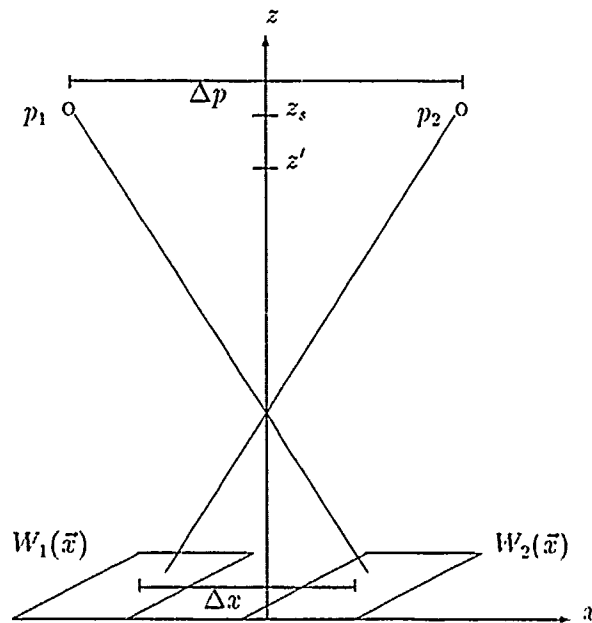


Figure 3.1. Measurement Geometry

in the aperture plane of the optical system. The wave front sensors are separated by the vector distance $\Delta \vec{x}$. Each sensor measures the slope of the distorted wave front across a finite area called a subaperture. Each sensor is divided into multiple subapertures, each of which provides a slope measurement.

It is common to normalize the aperture weighting functions (16:1771) so that

$$\int d^2\vec{x} W_n(\vec{x}) = 1 \quad (3.1)$$

where n , in the case of figure 3.1, may be 1 or 2.

The point sources are at a height z , above the aperture plane and z' is a point along the z axis. As can be seen from the figure, the geometric relationship between the sources and the sensors gives rise to crossed optical paths. The light from each point source travels a different optical path to the wave front sensor. At the point where the paths cross, the turbulence contributions will be highly correlated. This correlation is exploited to calculate C_n^2 .

This chapter contains mathematical derivations based on the correlation of wave front phase slopes for the geometry of figure 3.1. The first derivation proves that the correlation of wave front slopes, denoted C_s , can be related to C_n^2 by the following equation.

$$C_s = \int dz' C_n^2(z') w(z') \quad (3.2)$$

where z' is a position along the optical path and $w(z')$ is a path weighting function. If $w(z')$ has the shape of a Dirac delta function (i.e. a sampling function), the sifting property may be applied to equation 3.2 to directly relate C_s to C_n^2 .

Following the derivation of equation 3.2, the expression for $w(z')$ is simplified so that it depends only on terms of the measurement geometry (Δx , Δp , z' , etc.). This allows $w(z')$ to be plotted to examine the sampling characteristics. It is shown in Chapter 4 that the path weighting function derived in this chapter does not possess an ideal sampling shape. Therefore, a discussion is included in this chapter about a method to improve the shape of $w(z')$.

Finally, an expression for the signal-to-noise ratio of the correlation measurement is derived. This is used to quantify the accuracy of the measurement technique.

3.2 Overview of Derivation

Since the derivation of equation 3.2 is rather involved, it is useful to first outline the procedure. The first step is to define what is meant by the correlation of wave front slopes. The next step is to define an expression which relates the slope signals to the measurement geometry of figure 3.1. This allows the correlation of the wave front slopes to be directly related to the measurement geometry.

After the expression for the correlation of the wave front slopes is developed, the ensemble average is taken. This is done because the slope signals are defined in terms of the wave front phase of the optical wave from each source, which is a random process. Taking the ensemble average introduces the second order moment of the wave front phase. An expression in the literature relates the second order moment of the phase to the phase structure function. Recalling from Chapter 2 that the structure function is related to C_n^2 , the next step is to use an expression (also from the literature) to relate the two quantities. The resulting expression will be an integral over z' that includes C_n^2 and several other terms. The terms other than C_n^2 are grouped and called $w(z')$, the path weighting function.

The final part of the derivation concentrates on the path weighting function. By assuming Kolmogoroff statistics for the atmosphere, $w(z')$ is reduced to a form which is only dependent upon known quantities from the measurement geometry. It is therefore possible to plot $w(z')$ to examine how closely it approximates a sampling function.

3.3 Derivation of the Path Weighting Function

This section contains the derivation of the path weighting function denoted as $w(z')$ in equation 3.2.

3.3.1 Correlation of Slope Signals The first step is to define the correlation as

$$C_s(\Delta\vec{x}) = \langle s_1 s_2 \rangle \quad (3.3)$$

where s_1 and s_2 are the slope signals from two individual wave front sensor subapertures separated by Δx . Recalling the geometry of figure 3.1, s_1 is the slope measurement arising from reference source 1, and s_2 is the slope measurement arising from reference source 2. For the remainder of this development, it is assumed that each wave front sensor consists of only a single subaperture and the separation between the sensors is Δx .

The next step is to find an expression for the slope signal. Referring to the literature, (16:1771) the phase of the incoming wave is designated $\psi_n(\vec{x})$ where \vec{x} is a two-dimensional position vector and n refers to the source of the wave front. For the geometry of figure 3.1, n may be 1 or 2. It is convenient to define a zero mean phase (4:1914) related to $\psi_n(\vec{x})$ by

$$\phi_n(\vec{x}) = \psi_n(\vec{x}) - \int d^2\vec{x}' W_n(\vec{x}') \psi_n(\vec{x}') \quad (3.4)$$

The output of a wave front sensor is a noisy measurement of the average slope of $\phi_n(\vec{x})$ over the aperture and is designated s_n . The conditional mean for s_n is

$$s_n = \int d^2\vec{x} W_n(\vec{x}) [\nabla \phi_n(\vec{x}) \cdot \hat{d}_n] + \alpha_n \quad (3.5)$$

where $W_n(\vec{x})$ is the aperture weighting function, $\nabla \phi_n(\vec{x})$ is the spatial gradient of the phase ϕ_n , \hat{d}_n is a unit vector in the direction of sensitivity of the sensor, and α_n is the slope measurement error. The measurement error is attributed to photon noise in the detection process. Integration by parts yields

$$s_n = - \int d^2\vec{x} [\nabla W_n(\vec{x}) \cdot \hat{d}_n] \phi_n(\vec{x}) + \alpha_n \quad (3.6)$$

To simplify notation, let $\nabla W_n(\vec{x}) \cdot \hat{d}_n = W_n^s(\vec{x})$ where $W_n^s(\vec{x})$ is the gradient of $W_n(\vec{x})$ in the direction of the n^{th} sensor. Rewrite:

$$s_n = - \int d^2\vec{x} W_n^s(\vec{x}) \phi_n(\vec{x}) + \alpha_n \quad (3.7)$$

Assuming the subaperture weighting functions are identical except for being shifted relative to each other, it is possible to write $W_1(\vec{x}) = W(\vec{x})$ and $W_2(\vec{x}) = W(\vec{x} - \Delta\vec{x})$ where $W(\vec{x})$ is the subaperture weighting function. Using these representations and plugging equation 3.7 into equation 3.3,

$$C_s(\Delta\vec{x}) = \left\{ \int d^2\vec{x} W^s(\vec{x}) \phi_1(\vec{x}) + \alpha_1 \right\} \times \left\{ \int d^2\vec{x}' W^s(\vec{x}' - \Delta\vec{x}) \phi_2(\vec{x}') + \alpha_2 \right\} \quad (3.8)$$

After multiplying and regrouping, $C_s(\vec{\Delta x})$ becomes

$$\begin{aligned}
 C_s(\vec{\Delta x}) = & \int d^2 \vec{x} \int d^2 \vec{x}' W^s(\vec{x}) W^s(\vec{x}' - \vec{\Delta x}) [\phi_1(\vec{x}) \phi_2(\vec{x}')] \\
 & + \int d^2 \vec{x} W^s(\vec{x}) \phi_1(\vec{x}) \alpha_2 \\
 & + \int d^2 \vec{x}' W^s(\vec{x}' - \vec{\Delta x}) \phi_2(\vec{x}') \alpha_1 \\
 & + \alpha_1 \alpha_2
 \end{aligned} \tag{3.9}$$

3.3.2 Ensemble Average of C_s . As mentioned in the Overview equation 3.9 contains random quantities and it is therefore necessary to use statistical methods to proceed with the derivation. ϕ is a two dimensional random process. α is assumed to be a zero mean random variable independent of ϕ . Consider the ensemble average of $C_s(\vec{\Delta x})$, denoted with the angle brackets:

$$\begin{aligned}
 \langle C_s(\vec{\Delta x}) \rangle = & \int d^2 \vec{x} \int d^2 \vec{x}' W^s(\vec{x}) W^s(\vec{x}' - \vec{\Delta x}) \langle \phi_1(\vec{x}) \phi_2(\vec{x}') \rangle \\
 & + 0 \\
 & + 0 \\
 & + \langle \alpha_1 \alpha_2 \rangle
 \end{aligned} \tag{3.10}$$

Simplifying,

$$\begin{aligned}
 \langle C_s(\vec{\Delta x}) \rangle = & \int d^2 \vec{x} \int d^2 \vec{x}' W^s(\vec{x}) W^s(\vec{x}' - \vec{\Delta x}) \langle \phi_1(\vec{x}) \phi_2(\vec{x}') \rangle \\
 & + \langle \alpha_1 \alpha_2 \rangle
 \end{aligned} \tag{3.11}$$

Consider the correlation of the noise functions, $\langle \alpha_1 \alpha_2 \rangle$, in equation 3.11. Recall that α_1 and α_2 are noise from the wave front sensor measurements. In equation 29 of reference (16), Wallner expresses the correlation of slope measurement noises as

$$\langle \alpha_n \alpha_{n'} \rangle = \sigma^2 \delta(n - n') \tag{3.12}$$

where n and n' designate the wave front sensor subapertures, σ^2 is the photon noise density, and $\delta(n - n')$ is the Dirac delta function. Equation 3.12 indicates that for different subapertures (i.e. $n \neq n'$), $\langle \alpha_n \alpha_{n'} \rangle = 0$. For the geometry under consideration, the subapertures do not coincide and the noise term is zero. Wallner also derives (16:1773-1774) an expression for the second order moment of the phase, $\langle \phi_1(\vec{x}) \phi_2(\vec{x}') \rangle$, in terms of the phase structure function D_{12} :

$$\langle \phi_1(\vec{x}) \phi_2(\vec{x}') \rangle = -\frac{1}{2} D_{12}(\vec{x}, \vec{x}') + g(\vec{x}) + g(\vec{x}') - a \quad (3.13)$$

where

$$D_{12}(\vec{x}, \vec{x}') = \langle [\psi(\vec{x}) - \psi(\vec{x}')]^2 \rangle \quad (3.14)$$

and

$$g(\vec{x}) = \frac{1}{2} \int d\vec{x}'' W(\vec{x}'') D(\vec{x}, \vec{x}'') \quad (3.15)$$

and

$$a = \frac{1}{2} \int d\vec{x}'' \int d\vec{x}''' W(\vec{x}'') W(\vec{x}''') D(\vec{x}'', \vec{x}''') \quad (3.16)$$

Since $W^s(\vec{x})$ is an odd-symmetric function, the integration over \vec{x}'' and \vec{x}''' yield a zero value. Therefore, all terms in equation 3.13, except $-\frac{1}{2} D_{12}(\vec{x}, \vec{x}')$, will go to zero.

Using equations 3.13 and 3.12 in equation 3.11, the correlation of the slope signals may be written as

$$\langle C_s(\Delta \vec{x}) \rangle = \int d^2 \vec{x} \int d^2 \vec{x}' W^s(\vec{x}) W^s(\vec{x}' - \Delta \vec{x}) \left[-\frac{1}{2} D_{12}(\vec{x}, \vec{x}') \right] \quad (3.17)$$

To further simplify equation 3.17, it is necessary to have an expression for $D_{12}(\vec{x}, \vec{x}')$ that is applicable to atmospheric turbulence and the geometry of figure 3.1. This is discussed in the next section.

3.3.3 Path Weighting Function For spatially stationary, transverse isotropic turbulence for the two source geometry of figure 3.1, Lutomirski and Buser (11:2160) show that the phase structure function may be expressed as

$$D_{1,2}(\vec{x} - \vec{x}') = \quad (3.18)$$

$$8\pi^2 k^2 \int_0^{z_s} dz' \int_0^\infty dK_\perp K_\perp \Phi_n(K_\perp, 0, z')$$

$$\times \left\{ 1 - J_0 \left(K_\perp \left| (\vec{\Delta p}) \left(\frac{z'}{z_s} \right) + (\vec{x} - \vec{x}') \left(1 - \frac{z'}{z_s} \right) \right| \right) \right\}$$

where $\Phi_n(K_\perp, K_z, z')$ is the spectral density of the index of refraction, $\vec{\Delta p}$ is the vector separation of the optical sources, and x and x' specify two points in the aperture plane of the optical system. The spectral density, Φ_n , is a function of distance from the aperture plane, z' , and of wavenumber components perpendicular (K_\perp) and parallel (K_z) to the z axis. J_0 is the zero-order Bessel function.

Following Welsh (18), assume the power spectrum of the index of refraction is separable in the perpendicular and parallel wavenumber components (K_\perp, K_z) and z' . This yields

$$\Phi_n(K_\perp, K_z, z') = \Phi'_n(K_\perp, K_z) C_n^2(z') \quad (3.19)$$

Substituting equation 3.18 and 3.19 into equation 3.17 yields

$$\langle C_s(\vec{\Delta x}) \rangle = \quad (3.20)$$

$$\int d^2\vec{x} \int d^2\vec{x}' W^s(\vec{x}) W^s(\vec{x}' - \vec{\Delta x})$$

$$\times (-4\pi^2 k^2) \int_0^{z_s} dz' \int_0^\infty dK_\perp K_\perp \Phi'_n(K_\perp, 0) C_n^2(z')$$

$$\times \left\{ 1 - J_0 \left(K_\perp \left| (\vec{\Delta p}) \left(\frac{z'}{z_s} \right) + (\vec{x} - \vec{x}') \left(1 - \frac{z'}{z_s} \right) \right| \right) \right\}$$

To match the form of equation 3.2, this may be rewritten as

$$\langle C_s(\vec{\Delta x}) \rangle = \int_0^{z_s} dz' C_n^2(z') w(z', z_s, \vec{\Delta x}, \vec{\Delta p}) \quad (3.21)$$

where $w(z', z_s, \vec{\Delta x}, \vec{\Delta p})$ is a path weighting function and is defined as

$$\begin{aligned}
w(z', z_s, \vec{\Delta x}, \vec{\Delta p}) = & \quad (3.22) \\
& \int d^2 \vec{x} \int d^2 \vec{x}' W^s(\vec{x}) W^s(\vec{x}' - \vec{\Delta x}) \\
& \times (-4\pi^2 k^2) \int_0^\infty dK_\perp K_\perp \Phi'_n(K_\perp, 0) \\
& \times \left\{ 1 - J_0 \left(K_\perp \left| (\vec{\Delta p}) \left(\frac{z'}{z_s} \right) + (\vec{x} - \vec{x}') \left(1 - \frac{z'}{z_s} \right) \right| \right) \right\}
\end{aligned}$$

3.3.4 Evaluation of Path Weighting Function To further evaluate the path weighting function, it is necessary to assume a form for Φ'_n . For atmospheric turbulence, Kolmogoroff (9:154) has shown that

$$\Phi'_n(K_\perp, K_z) = 0.033 K^{-\frac{11}{3}} \quad (3.23)$$

where $K = |K_\perp + K_z|$. Using 3.23, the expression for the path weighting function may be rewritten as

$$\begin{aligned}
w(z', z_s, \vec{\Delta x}, \vec{\Delta p}) = & \quad (3.24) \\
& -4\pi^2 k^2 \int d^2 \vec{x} \int d^2 \vec{x}' W^s(\vec{x}) W^s(\vec{x}' - \vec{\Delta x}) \\
& \times \int_0^\infty dK_\perp K_\perp 0.033 K^{-\frac{11}{3}} \\
& \times \left\{ 1 - J_0 \left(K_\perp \left| (\vec{\Delta p}) \left(\frac{z'}{z_s} \right) + (\vec{x} - \vec{x}') \left(1 - \frac{z'}{z_s} \right) \right| \right) \right\}
\end{aligned}$$

Employing the integral identity (15:269)

$$\int_0^\infty dx (1 - J_0)x^{-p} = \pi \left\{ 2^p \left[\Gamma\left(\frac{p+1}{2}\right) \right]^2 \sin \frac{\pi(p-1)}{2} \right\}^{-1} \quad (3.25)$$

where $1 < p < 3$, and combining terms,

$$\begin{aligned}
w(z', z_s, \vec{\Delta x}, \vec{\Delta p}) = & \quad (3.26) \\
& -4(0.033)\pi^2 k^2 \int d^2 \vec{x} \int d^2 \vec{x}' W_1^s(\vec{x}) W_2^s(\vec{x}' - \vec{\Delta x}) \\
& \times \pi \left[2^{\frac{5}{2}} \Gamma^2\left(\frac{11}{6}\right) \sin\left(\frac{5\pi}{6}\right) \right]^{-1} \\
& \times \left| (\vec{\Delta p}) \left(\frac{z'}{z_s} \right) + (\vec{x} - \vec{x}') \left(1 - \frac{z'}{z_s} \right) \right|^{\frac{5}{2}}
\end{aligned}$$

Simplifying,

$$w(z', z_s, \vec{\Delta x}, \vec{\Delta p}) = \quad (3.27)$$

$$-1.46k^2 \int d^2 \vec{x} \int d^2 \vec{x}' W^s(\vec{x}) W^s(\vec{x}' - \vec{\Delta x})$$

$$\times \left| (\vec{\Delta p}) \left(\frac{z'}{z_s} \right) + (\vec{x} - \vec{x}') \left(1 - \frac{z'}{z_s} \right) \right|^{\frac{2}{3}}$$

To evaluate equation 3.27, it is necessary to assume an expression for $W^s(\vec{x})$. It is not uncommon to see square subapertures in a wave front sensor and the rectangle function is commonly used to describe the transmittance of such an aperture (5:67). Mathematically, this implies that

$$W(\vec{x}) = \frac{1}{L^2} \text{rect}\left(\frac{x}{L}\right) \text{rect}\left(\frac{y}{L}\right) \quad (3.28)$$

where the factor $\frac{1}{L^2}$ is necessary to achieve normalization to 1 (see equation 3.1). Taking the derivative of equation 3.28 yields $W^s(\vec{x})$, as required.

In general, the derivative may be expressed using the delta function (5:63-66):

$$W^s(\vec{x}) = \nabla W(\vec{x}) \cdot \hat{d} = \frac{1}{L^2} \left[\delta\left(x + \frac{L}{2}\right) - \delta\left(x - \frac{L}{2}\right) \right] \text{rect}\left(\frac{y}{L}\right) \quad (3.29)$$

Implicit in this expression is the fact that the slope in the x direction is the quantity under consideration (i.e. \hat{d} is an x directed unit vector).

3.3.4.1 Evaluation of Absolute Value Quantity It is convenient at this point to evaluate the absolute value quantity in equation 3.27. Representing the vectors by their components in the \hat{x} and \hat{y} directions

$$\vec{\Delta p} = \Delta p_x \hat{x} + \Delta p_y \hat{y}, \quad (3.30)$$

$$\vec{\Delta x} = \Delta x \hat{x} + \Delta y \hat{y}, \quad (3.31)$$

$$\vec{x} = x \hat{x} + y \hat{y} \quad (3.32)$$

$$\vec{x}' = x' \hat{x} + y' \hat{y} \quad (3.33)$$

and substituting into equation 3.27 yields,

$$f(x, x', y, y', \Delta p_x, \Delta p_y, z', z_s) = \left| (\Delta p_x \hat{x} + \Delta p_y \hat{y}) \frac{z'}{z_s} + [x\hat{x} + y\hat{y} - (x'\hat{x} + y'\hat{y})] \left(1 - \frac{z'}{z_s}\right) \right|^2 \quad (3.34)$$

Simplifying,

$$f(x, x', y, y', \Delta p_x, \Delta p_y, z', z_s) = \left\{ \left[\Delta p_x \frac{z'}{z_s} + (x - x') \left(1 - \frac{z'}{z_s}\right) \right]^2 + \left[\Delta p_y \frac{z'}{z_s} + (y - y') \left(1 - \frac{z'}{z_s}\right) \right]^2 \right\} \quad (3.35)$$

Typically, z_s is much greater than z' over the range of interest. This is easily seen if the sources are laser guidestars. The guidestar altitude would be in the range of 90 to 100 kilometers. Recalling figure 2.1, the range of interest for the turbulence is well below this altitude. Therefore, $\frac{z'}{z_s}$ is much less than 1 and it is reasonable to use the approximation $(1 - \frac{z'}{z_s}) \approx 1$ and simplify:

$$f(x, x', y, y', \Delta p_x, \Delta p_y, z', z_s) = \left\{ \left[\Delta p_x \frac{z'}{z_s} + x - x' \right]^2 + \left[\Delta p_y \frac{z'}{z_s} + y - y' \right]^2 \right\} \quad (3.36)$$

3.3.5 Simplification of Path Weighting Function It is now possible to simplify the path weighting function in equation 3.27. Replacing the aperture functions with their mathematical representations,

$$w(z', z_s, \tilde{\Delta x}, \tilde{\Delta p}) = -1.46k^2 \int d^2 \tilde{x} \int d^2 \tilde{x}' f(x, x', y, y', \Delta p_x, \Delta p_y, z', z_s) \times \left\{ \frac{1}{L^2} [\delta(x + \frac{L}{2}) - \delta(x - \frac{L}{2})] \text{rect}(\frac{y}{L}) \right\} \times \left\{ \frac{1}{L^2} [\delta(x' - \Delta x + \frac{L}{2}) - \delta(x' - \Delta x - \frac{L}{2})] \text{rect}(\frac{y' + \Delta y}{L}) \right\} \quad (3.37)$$

where $f(x, x', y, y', \Delta p_x, \Delta p_y, z', z_s)$ is defined by equation 3.36. Employing the sifting property of the Dirac delta function allows the integrations over x and x' to be performed and the weighting function reduces to

$$\begin{aligned}
w(z', z_s, \vec{\Delta x}, \vec{\Delta p}) = & \quad (3.38) \\
& -1.46k^2 L^{-4} \int dy \operatorname{rect}\left(\frac{y}{L}\right) \int dy' \operatorname{rect}\left(\frac{y' + \Delta y}{L}\right) \times \\
& f\left(\frac{-L}{2}, \Delta x - \frac{L}{2}, y, y', \Delta p_x, \Delta p_y, z', z_s\right) - \\
& f\left(\frac{-L}{2}, \Delta x + \frac{L}{2}, y, y', \Delta p_x, \Delta p_y, z', z_s\right) - \\
& f\left(\frac{L}{2}, \Delta x - \frac{L}{2}, y, y', \Delta p_x, \Delta p_y, z', z_s\right) + \\
& f\left(\frac{L}{2}, \Delta x + \frac{L}{2}, y, y', \Delta p_x, \Delta p_y, z', z_s\right)
\end{aligned}$$

Let

$$\begin{aligned}
g(y - y') = & \quad (3.39) \\
& f\left(\frac{-L}{2}, \Delta x - \frac{L}{2}, y, y', \Delta p_x, \Delta p_y, z', z_s\right) - \\
& f\left(\frac{-L}{2}, \Delta x + \frac{L}{2}, y, y', \Delta p_x, \Delta p_y, z', z_s\right) - \\
& f\left(\frac{L}{2}, \Delta x - \frac{L}{2}, y, y', \Delta p_x, \Delta p_y, z', z_s\right) + \\
& f\left(\frac{L}{2}, \Delta x + \frac{L}{2}, y, y', \Delta p_x, \Delta p_y, z', z_s\right)
\end{aligned}$$

where dependence of g on $L, \Delta p_x, \Delta p_y, z',$ and z_s is dropped for notational convenience. Substituting 3.39 into 3.38 gives

$$\begin{aligned}
w(z', z_s, \vec{\Delta x}, \vec{\Delta p}) = & \quad (3.40) \\
& -1.46k^2 L^{-4} \int dy \operatorname{rect}\left(\frac{y}{L}\right) \int dy' \operatorname{rect}\left(\frac{y' - \Delta y}{L}\right) g(y - y')
\end{aligned}$$

By making the change of variables $u = y - y'$ and $v = \frac{y+y'}{2}$ equation 3.40 can be rewritten as

$$\begin{aligned}
w(z', z_s, \vec{\Delta x}, \vec{\Delta p}) = & \quad (3.41) \\
& -1.46k^2 L^{-4} \int du \int dv \operatorname{rect}\left(\frac{v + \frac{u}{2}}{L}\right) \operatorname{rect}\left(\frac{v - \frac{u}{2} - \Delta y}{L}\right) g(u)
\end{aligned}$$

Another change of variables results in

$$w(z', z_s, \vec{\Delta x}, \vec{\Delta p}) = -1.46k^2 L^{-4} \int du g(u) \int dv' \text{rect}\left(\frac{v'}{L}\right) \text{rect}\left(\frac{v' - u - \Delta y}{L}\right) \quad (3.42)$$

Evaluating the integral over v' yields

$$w(z', z_s, \vec{\Delta x}, \vec{\Delta p}) = -1.46k^2 L^{-3} \int du g(u) \text{tri}\left(\frac{u + \Delta y}{L}\right) \quad (3.43)$$

where tri is the triangle function. Using equations 3.39 and 3.36 the weighting function can be written

$$\begin{aligned} w(z', z_s, \vec{\Delta x}, \vec{\Delta p}) = & -1.46k^2 L^{-3} \int du \text{tri}\left(\frac{u + \Delta y}{L}\right) \times \\ & 2 \left[\left(\Delta p_x \frac{z'}{z_s} - \Delta x \right)^2 + \left(\Delta p_y \frac{z'}{z_s} + u \right)^2 \right]^{\frac{5}{8}} \\ & - \left[\left(\Delta p_x \frac{z'}{z_s} - \Delta x - L \right)^2 + \left(\Delta p_y \frac{z'}{z_s} + u \right)^2 \right]^{\frac{5}{8}} \\ & - \left[\left(\Delta p_x \frac{z'}{z_s} - \Delta x + L \right)^2 + \left(\Delta p_y \frac{z'}{z_s} + u \right)^2 \right]^{\frac{5}{8}} \end{aligned} \quad (3.44)$$

Without loss of generality, assume the apertures and point source geometry is such that there is no offset in the y direction. This implies Δy and Δp_y are 0 and equation 3.44 simplifies to

$$\begin{aligned} w(z', z_s, \Delta x, \Delta p) = & -1.46k^2 L^{-3} \int du \text{tri}\left(\frac{u}{L}\right) \times \\ & 2 \left[\left(\Delta p_x \frac{z'}{z_s} - \Delta x \right)^2 + u^2 \right]^{\frac{5}{8}} \\ & - \left[\left(\Delta p_x \frac{z'}{z_s} - \Delta x - L \right)^2 + u^2 \right]^{\frac{5}{8}} \\ & - \left[\left(\Delta p_x \frac{z'}{z_s} - \Delta x + L \right)^2 + u^2 \right]^{\frac{5}{8}} \end{aligned} \quad (3.45)$$

The quantity $\Delta p_x \frac{z'}{z_s} - \Delta x$ may be interpreted as the vector distance between the crossed ray paths as a function of z' (see figure 3.1). Let $p = \Delta p_x \frac{z'}{z_s} - \Delta x$ and rewrite as

$$w(z', z_s, \Delta x, \Delta p) = \quad (3.46)$$

$$-1.46k^2 L^{-3} \int du \operatorname{tri}\left(\frac{u}{L}\right) \times$$

$$\left\{ 2 [p^2 + u^2]^{\frac{5}{6}} - [(p-L)^2 + u^2]^{\frac{5}{6}} - [(p+L)^2 + u^2]^{\frac{5}{6}} \right\}$$

Let $u' = \frac{u}{L}$. This allows the integral to become dimensionless and the integration may be performed from -1 to 1 , regardless of the size of L . To simplify notation, the weighting function is designated as $w(z')$ and is written as:

$$w(z') = \quad (3.47)$$

$$-1.46k^2 L^{-\frac{1}{3}} \int_{-1}^1 du' \operatorname{tri}(u') \times$$

$$\left\{ 2 \left[\left(\frac{p}{L} \right)^2 + u'^2 \right]^{\frac{5}{6}} - \left[\left(\frac{p}{L} - 1 \right)^2 + u'^2 \right]^{\frac{5}{6}} - \left[\left(\frac{p}{L} + 1 \right)^2 + u'^2 \right]^{\frac{5}{6}} \right\}$$

This is the final expression for the path weighting function. The characteristics of this function are examined in the next chapter.

3.4 Improvement of the Path Weighting Function

It is shown in the next chapter that the shape of the path weighting function derived in the previous section does not possess the characteristics of a sampling function. The low spatial frequencies of the phase perturbations are causing a common tilt in both slope measurements. This effect shows up as a dc offset in the weighting function. The method used to improve the shape of the path weighting function is to combine the measurements for different size apertures. This action should remove the common tilt component. Equation 3.47 is used with different values of L to achieve the desired result. Plots of the improved weighting function for this method are given in the next chapter.

3.5 Signal-to-Noise Ratio of the Correlation Measurement

In order to quantify the usefulness of the techniques developed in this research, the signal-to-noise ratio (SNR) of the correlation measurement C_s is calculated. In general, the SNR may be expressed as (20:170-171)

$$SNR = \frac{\langle C_s(\vec{\Delta x}) \rangle}{[\langle C_s^2(\vec{\Delta x}) \rangle - \langle C_s(\vec{\Delta x}) \rangle^2]^{\frac{1}{2}}} \quad (3.48)$$

where the quantity in the denominator is recognized as the square root of the variance (i.e. the standard deviation). The derivation of the variance is rather lengthy, however, the procedure is very similar to that followed in the beginning of this chapter. For that reason, the derivation of the expression for the variance is summarized in the following section.

3.5.1 Derivation of the Variance The variance of C_s is given by the square of the denominator of equation 3.47

$$VAR = \langle C_s^2(\vec{\Delta}x) \rangle - \langle C_s(\vec{\Delta}x) \rangle^2 \quad (3.49)$$

The second term on the right hand side of equation 3.49 is the square of the already derived result given by equations 3.21 and 3.47. The first term on the right hand side is the ensemble average of the square of C_s . To calculate this first term, equation 3.9 is squared and the ensemble average is taken. Squaring equation 3.9 yields 16 terms. However, α is a zero mean random process and 12 terms go to zero when the ensemble average is taken. Equation 3.49 may thus be written as:

$$\begin{aligned} VAR = & \quad (3.50) \\ & \int \int \int \int d^2\vec{x} d^2\vec{x}' d^2\vec{x}'' d^2\vec{x}''' \\ & \quad \times W^s(\vec{x}) W^s(\vec{x}') W^s(\vec{x}'' - \vec{\Delta}x) W^s(\vec{x}''' - \vec{\Delta}x) \\ & \quad \times \langle \phi_1(\vec{x}) \phi_2(\vec{x}') \phi_3(\vec{x}'') \phi_4(\vec{x}''') \rangle \\ & + \int \int d^2\vec{x} d^2\vec{x}' W^s(\vec{x}) W^s(\vec{x}') \langle \phi_1(\vec{x}) \phi_2(\vec{x}') \rangle \langle \alpha_1 \alpha_1 \rangle \\ & + \int \int d^2\vec{x}'' d^2\vec{x}''' W^s(\vec{x}'' - \vec{\Delta}x) W^s(\vec{x}''' - \vec{\Delta}x) \langle \phi_3(\vec{x}'') \phi_4(\vec{x}''') \rangle \langle \alpha_2 \alpha_2 \rangle \\ & + \langle \alpha_1 \alpha_1 \rangle \langle \alpha_2 \alpha_2 \rangle \\ & - \left[\int \int d^2\vec{x} d^2\vec{x}' W^s(\vec{x}) W^s(\vec{x}') \langle \phi_1(\vec{x}) \phi_2(\vec{x}') \rangle \right]^2 \end{aligned}$$

The reader will notice equation 3.50 is similar to equation 3.10. The fundamental difference is the presence of the fourth order moment of the phase rather than the second order moment. Calculation of the fourth order moment of the phase is possible if Gaussian

statistics are assumed since, for Gaussian processes, the fourth order moment may be expressed as a combination of the first and second order moments (6:39). Using the Gaussian assumption, the variance expression takes the following form:

$$VAR = \quad (3.51)$$

$$\begin{aligned} & 2.13 k^4 L^{-6} \int_0^{z_s} \int_0^{z_s} dz' dz'' C_n^2(z') C_n^2(z'') \\ & \times \int du \operatorname{tri}\left(\frac{u}{L}\right) \int dv \operatorname{tri}\left(\frac{v}{L}\right) [f_1(u, v, z', z'') + 2f_2(u, v, z', z'')] \\ & + 1.46 k^4 \sigma^2 L^{-3} \int_0^{z_s} dz' C_n^2(z') \int du \operatorname{tri}\left(\frac{u}{L}\right) 2f_3(u, z') \\ & + \sigma^4 \\ & - \left[1.46 k^2 L^{-3} \int_0^{z_s} dz' C_n^2(z') \int du \operatorname{tri}\left(\frac{u}{L}\right) f_4(u, z') \right]^2 \end{aligned}$$

The functions f_1 to f_4 are similar in form to g of equation 3.39. Letting p equal $\Delta p_x \frac{z'}{z_s}$, the functions are as follows.

$$f_1(u, v, z', z'') = \quad (3.52)$$

$$\begin{aligned} & 4 \left[(\Delta p_x \frac{z'}{z_s})^2 + u^2 \right]^{\frac{5}{6}} \left[(\Delta p_x \frac{z''}{z_s})^2 + v^2 \right]^{\frac{5}{6}} \\ & - 2 \left[(\Delta p_x \frac{z'}{z_s} + L)^2 + u^2 \right]^{\frac{5}{6}} \left[(\Delta p_x \frac{z''}{z_s})^2 + v^2 \right]^{\frac{5}{6}} \\ & - 2 \left[(\Delta p_x \frac{z'}{z_s})^2 + u^2 \right]^{\frac{5}{6}} \left[(\Delta p_x \frac{z''}{z_s} - L)^2 + v^2 \right]^{\frac{5}{6}} \\ & - 2 \left[(\Delta p_x \frac{z'}{z_s})^2 + u^2 \right]^{\frac{5}{6}} \left[(\Delta p_x \frac{z''}{z_s} + L)^2 + v^2 \right]^{\frac{5}{6}} \\ & - 2 \left[(\Delta p_x \frac{z'}{z_s} - L)^2 + u^2 \right]^{\frac{5}{6}} \left[(\Delta p_x \frac{z''}{z_s})^2 + v^2 \right]^{\frac{5}{6}} \\ & + \left[(\Delta p_x \frac{z'}{z_s} + L)^2 + u^2 \right]^{\frac{5}{6}} \left[(\Delta p_x \frac{z''}{z_s} + L)^2 + v^2 \right]^{\frac{5}{6}} \\ & + \left[(\Delta p_x \frac{z'}{z_s} + L)^2 + u^2 \right]^{\frac{5}{6}} \left[(\Delta p_x \frac{z''}{z_s} - L)^2 + v^2 \right]^{\frac{5}{6}} \\ & + \left[(\Delta p_x \frac{z'}{z_s} - L)^2 + u^2 \right]^{\frac{5}{6}} \left[(\Delta p_x \frac{z''}{z_s} + L)^2 + v^2 \right]^{\frac{5}{6}} \end{aligned}$$

$$+ \left[\left(\Delta p_x \frac{z'}{z_s} - L \right)^2 + u^2 \right]^{\frac{5}{6}} \left[\left(\Delta p_x \frac{z''}{z_s} - L \right)^2 + v^2 \right]^{\frac{5}{6}}$$

$$f_2(u, v, z', z'') = \quad (3.53)$$

$$\begin{aligned} & 4 \left[\left(\Delta p_x \frac{z'}{z_s} - \Delta x \right)^2 + u^2 \right]^{\frac{5}{6}} \left[\left(\Delta p_x \frac{z''}{z_s} - \Delta x \right)^2 + v^2 \right]^{\frac{5}{6}} \\ & - 2 \left[\left(\Delta p_x \frac{z'}{z_s} - \Delta x + L \right)^2 + u^2 \right]^{\frac{5}{6}} \left[\left(\Delta p_x \frac{z''}{z_s} - \Delta x \right)^2 + v^2 \right]^{\frac{5}{6}} \\ & - 2 \left[\left(\Delta p_x \frac{z'}{z_s} - \Delta x \right)^2 + u^2 \right]^{\frac{5}{6}} \left[\left(\Delta p_x \frac{z''}{z_s} - \Delta x + L \right)^2 + v^2 \right]^{\frac{5}{6}} \\ & - 2 \left[\left(\Delta p_x \frac{z'}{z_s} - \Delta x - L \right)^2 + u^2 \right]^{\frac{5}{6}} \left[\left(\Delta p_x \frac{z''}{z_s} - \Delta x \right)^2 + v^2 \right]^{\frac{5}{6}} \\ & - 2 \left[\left(\Delta p_x \frac{z'}{z_s} - \Delta x \right)^2 + u^2 \right]^{\frac{5}{6}} \left[\left(\Delta p_x \frac{z''}{z_s} - \Delta x - L \right)^2 + v^2 \right]^{\frac{5}{6}} \\ & + \left[\left(\Delta p_x \frac{z'}{z_s} - \Delta x + L \right)^2 + u^2 \right]^{\frac{5}{6}} \left[\left(\Delta p_x \frac{z''}{z_s} - \Delta x + L \right)^2 + v^2 \right]^{\frac{5}{6}} \\ & + \left[\left(\Delta p_x \frac{z'}{z_s} - \Delta x + L \right)^2 + u^2 \right]^{\frac{5}{6}} \left[\left(\Delta p_x \frac{z''}{z_s} - \Delta x - L \right)^2 + v^2 \right]^{\frac{5}{6}} \\ & + \left[\left(\Delta p_x \frac{z'}{z_s} - \Delta x - L \right)^2 + u^2 \right]^{\frac{5}{6}} \left[\left(\Delta p_x \frac{z''}{z_s} - \Delta x + L \right)^2 + v^2 \right]^{\frac{5}{6}} \\ & + \left[\left(\Delta p_x \frac{z'}{z_s} - \Delta x - L \right)^2 + u^2 \right]^{\frac{5}{6}} \left[\left(\Delta p_x \frac{z''}{z_s} - \Delta x - L \right)^2 + v^2 \right]^{\frac{5}{6}} \end{aligned}$$

$$f_3(u, z') = \quad (3.54)$$

$$\begin{aligned} & 2 \left[\left(\Delta p_x \frac{z'}{z_s} \right)^2 + u^2 \right]^{\frac{5}{6}} \\ & - \left[\left(\Delta p_x \frac{z'}{z_s} - L \right)^2 + u^2 \right]^{\frac{5}{6}} \\ & - \left[\left(\Delta p_x \frac{z'}{z_s} + L \right)^2 + u^2 \right]^{\frac{5}{6}} \end{aligned}$$

$$f_4(u, z') = \frac{1}{2} \left[\left(\Delta p_x \frac{z'}{z_s} - \Delta x \right)^2 + u^2 \right]^{\frac{5}{2}} - \left[\left(\Delta p_x \frac{z'}{z_s} - \Delta x - L \right)^2 + u^2 \right]^{\frac{5}{2}} - \left[\left(\Delta p_x \frac{z'}{z_s} - \Delta x + L \right)^2 + u^2 \right]^{\frac{5}{2}} \quad (3.55)$$

At this point, in order to get some simplified results, it is necessary to assume a form for the turbulence. The assumption is made that the turbulence is confined to two layers. This is represented by

$$C_n^2(z) = C_{n_1}^2 \delta(z - z_1) + C_{n_2}^2 \delta(z - z_2) \quad (3.56)$$

Using this form for C_n^2 , the sifting property of the delta function is employed to remove the integrals over z' and z'' . The expression for the variance is now reduced to

$$\begin{aligned} VAR = & \quad (3.57) \\ & 2.13k^4 C_{n_1}^2 C_{n_2}^2 L^{-6} \int \int du dv \operatorname{tri}\left(\frac{u}{L}\right) \operatorname{tri}\left(\frac{v}{L}\right) \\ & \quad \times [f_1(u, v) + 2f_2(u, v)] \\ & + 2.92k^2 \sigma^2 C_{n_1}^2 L^{-3} \int du \operatorname{tri}\left(\frac{u}{L}\right) f_3(u) \\ & + 2.92k^2 \sigma^2 C_{n_2}^2 L^{-3} \int du \operatorname{tri}\left(\frac{u}{L}\right) f_4(u) \\ & + \sigma^4 \\ & - \left[1.46k^2 C_{n_1}^2 L^{-3} \int du \operatorname{tri}\left(\frac{u}{L}\right) f_5(u) \right. \\ & \quad \left. + 1.46k^2 C_{n_2}^2 L^{-3} \int du \operatorname{tri}\left(\frac{u}{L}\right) f_6(u) \right]^2 \end{aligned}$$

There are now six functions (f_1 to f_6) instead of four. This is because the existence of two layers of turbulence causes the second and fourth integrals in equation 3.50 to each split into two integrals, one involving $C_{n_1}^2$ and one involving $C_{n_2}^2$. The six functions are in

terms of $p_1 = \Delta p_x \frac{z_1}{z_0}$, $p_2 = \Delta p_x \frac{z_2}{z_0}$, $p_3 = p_1 - \Delta x$, and $p_4 = p_2 - \Delta x$. They are

$$f_1(u, v) = \quad (3.58)$$

$$\begin{aligned} & 4 [p_1^2 + u^2]^{\frac{5}{8}} [p_1^2 + v^2]^{\frac{5}{8}} \\ & -2 [(p_1 + L)^2 + u^2]^{\frac{5}{8}} [p_1^2 + v^2]^{\frac{5}{8}} \\ & -2 [p_1^2 + u^2]^{\frac{5}{8}} [(p_1 - L)^2 + v^2]^{\frac{5}{8}} \\ & -2 [p_1^2 + u^2]^{\frac{5}{8}} [(p_1 + L)^2 + v^2]^{\frac{5}{8}} \\ & -2 [(p_1 - L)^2 + u^2]^{\frac{5}{8}} [p_1^2 + v^2]^{\frac{5}{8}} \\ & + [(p_1 + L)^2 + u^2]^{\frac{5}{8}} [(p_1 + L)^2 + v^2]^{\frac{5}{8}} \\ & + [(p_1 + L)^2 + u^2]^{\frac{5}{8}} [(p_1 - L)^2 + v^2]^{\frac{5}{8}} \\ & + [(p_1 - L)^2 + u^2]^{\frac{5}{8}} [(p_1 + L)^2 + v^2]^{\frac{5}{8}} \\ & + [(p_1 - L)^2 + u^2]^{\frac{5}{8}} [(p_1 - L)^2 + v^2]^{\frac{5}{8}} \\ & +4 [p_1^2 + u^2]^{\frac{5}{8}} [p_2^2 + v^2]^{\frac{5}{8}} \\ & -2 [(p_1 + L)^2 + u^2]^{\frac{5}{8}} [p_2^2 + v^2]^{\frac{5}{8}} \\ & -2 [p_1^2 + u^2]^{\frac{5}{8}} [(p_2 - L)^2 + v^2]^{\frac{5}{8}} \\ & -2 [p_1^2 + u^2]^{\frac{5}{8}} [(p_2 + L)^2 + v^2]^{\frac{5}{8}} \\ & -2 [(p_1 - L)^2 + u^2]^{\frac{5}{8}} [p_2^2 + v^2]^{\frac{5}{8}} \\ & + [(p_1 + L)^2 + u^2]^{\frac{5}{8}} [(p_2 + L)^2 + v^2]^{\frac{5}{8}} \\ & + [(p_1 + L)^2 + u^2]^{\frac{5}{8}} [(p_2 - L)^2 + v^2]^{\frac{5}{8}} \\ & + [(p_1 - L)^2 + u^2]^{\frac{5}{8}} [(p_2 + L)^2 + v^2]^{\frac{5}{8}} \\ & + [(p_1 - L)^2 + u^2]^{\frac{5}{8}} [(p_2 - L)^2 + v^2]^{\frac{5}{8}} \\ & +4 [p_2^2 + u^2]^{\frac{5}{8}} [p_1^2 + v^2]^{\frac{5}{8}} \\ & -2 [(p_2 + L)^2 + u^2]^{\frac{5}{8}} [p_1^2 + v^2]^{\frac{5}{8}} \\ & -2 [p_2^2 + u^2]^{\frac{5}{8}} [(p_1 - L)^2 + v^2]^{\frac{5}{8}} \\ & -2 [p_2^2 + u^2]^{\frac{5}{8}} [(p_1 + L)^2 + v^2]^{\frac{5}{8}} \\ & -2 [(p_2 - L)^2 + u^2]^{\frac{5}{8}} [p_1^2 + v^2]^{\frac{5}{8}} \\ & + [(p_2 + L)^2 + u^2]^{\frac{5}{8}} [(p_1 + L)^2 + v^2]^{\frac{5}{8}} \\ & + [(p_2 + L)^2 + u^2]^{\frac{5}{8}} [(p_1 - L)^2 + v^2]^{\frac{5}{8}} \\ & + [(p_2 - L)^2 + u^2]^{\frac{5}{8}} [(p_1 + L)^2 + v^2]^{\frac{5}{8}} \\ & + [(p_2 - L)^2 + u^2]^{\frac{5}{8}} [(p_1 - L)^2 + v^2]^{\frac{5}{8}} \end{aligned}$$

$$\begin{aligned}
& +4 [p_2^2 + u^2]^{\frac{5}{6}} [p_2^2 + v^2]^{\frac{5}{6}} \\
& -2 [(p_2 + L)^2 + u^2]^{\frac{5}{6}} [p_2^2 + v^2]^{\frac{5}{6}} \\
& -2 [p_2^2 + u^2]^{\frac{5}{6}} [(p_2 - L)^2 + v^2]^{\frac{5}{6}} \\
& -2 [p_2^2 + u^2]^{\frac{5}{6}} [(p_2 + L)^2 + v^2]^{\frac{5}{6}} \\
& -2 [(p_2 - L)^2 + u^2]^{\frac{5}{6}} [p_2^2 + v^2]^{\frac{5}{6}} \\
& + [(p_2 + L)^2 + u^2]^{\frac{5}{6}} [(p_2 + L)^2 + v^2]^{\frac{5}{6}} \\
& + [(p_2 + L)^2 + u^2]^{\frac{5}{6}} [(p_2 - L)^2 + v^2]^{\frac{5}{6}} \\
& + [(p_2 - L)^2 + u^2]^{\frac{5}{6}} [(p_2 + L)^2 + v^2]^{\frac{5}{6}} \\
& + [(p_2 - L)^2 + u^2]^{\frac{5}{6}} [(p_2 - L)^2 + v^2]^{\frac{5}{6}}
\end{aligned}$$

The function $f_2(u, v)$ has the same form as $f_1(u, v)$ except the p_1 is replaced by p_3 and the p_2 is replaced by p_4 . The remaining functions are

$$\begin{aligned}
f_3(u) = & \quad (3.59) \\
& 2 [p_1^2 + u^2]^{\frac{5}{6}} - [(p_1 - L)^2 + u^2]^{\frac{5}{6}} - [(p_1 + L)^2 + u^2]^{\frac{5}{6}}
\end{aligned}$$

$f_4(u) = f_3(u)$ with p_1 replaced by p_2 .

$$\begin{aligned}
f_5(u) = & \quad (3.60) \\
& 2 [p_3^2 + u^2]^{\frac{5}{6}} - [(p_3 - L)^2 + u^2]^{\frac{5}{6}} - [(p_3 + L)^2 + u^2]^{\frac{5}{6}}
\end{aligned}$$

$f_6(u) = f_5(u)$ with p_3 replaced by p_4 .

3.5.2 Reduction of the Variance Expression In atmospheric optics, the atmospheric coherence diameter, r_0 , is a commonly encountered parameter. In a diffraction limited system using a long exposure, the resolution will increase with aperture size. However, the resolution will reach a limiting value beyond which an increase in aperture size will not affect resolution. The limiting value is known as the atmospheric coherence diameter (6:429-439). It is often thought of as a measure of how good the 'seeing' is at any given time. To make the expression for the variance (and hence the SNR) more meaningful, it is helpful to relate it to r_0 . Goodman (6:431) provides an expression for r_0 :

$$r_0 = 0.185 \left[\frac{\lambda^2}{\int_0^z C_n^2(\xi) d\xi} \right]^{\frac{3}{5}} \quad (3.61)$$

Using the assumption of two-layer turbulence, the integral expression in the denominator may be replaced by $C_{n_1}^2 + C_{n_2}^2$. Replacing λ by $\frac{2\pi}{k}$ and factoring out an L from each of the terms in the integrals, equation 3.57 may be written in terms of dimensionless integrals as follows:

$$VAR = \quad (3.62)$$

$$\begin{aligned} & 11.98 \left(\frac{L}{r_0} \right)^{\frac{10}{3}} L^{-4} \left[\frac{C_{n_1}^2}{C_{n_2}^2} + \frac{C_{n_2}^2}{C_{n_1}^2} \right]^{-1} \int_{-1}^1 \int_{-1}^1 du' dv' \text{tri}(u') \text{tri}(v') \\ & \quad [f'_1(u', v') + f'_2(u', v') + f'_3(u', v')] \\ & + 6.92 \left(\frac{L}{r_0} \right)^{\frac{8}{3}} L^{-2} \sigma^2 \left[1 + \frac{C_{n_2}^2}{C_{n_1}^2} \right]^{-1} \int_{-1}^1 du \text{tri}(u) f'_4(u) \\ & + 6.92 \left(\frac{L}{r_0} \right)^{\frac{8}{3}} L^{-2} \sigma^2 \left[1 + \frac{C_{n_1}^2}{C_{n_2}^2} \right]^{-1} \int_{-1}^1 du' \text{tri}(u') f'_5(u') \\ & + \sigma^4 \\ & - \left[3.46 \left(\frac{L}{r_0} \right)^{\frac{8}{3}} L^{-2} \left[1 + \frac{C_{n_2}^2}{C_{n_1}^2} \right]^{-1} \int_{-1}^1 du' \text{tri}(u') f'_6(u') \right. \\ & \quad \left. + 3.46 \left(\frac{L}{r_0} \right)^{\frac{8}{3}} L^{-2} \left[1 + \frac{C_{n_1}^2}{C_{n_2}^2} \right]^{-1} \int_{-1}^1 du' \text{tri}(u') f'_7(u') \right]^2 \end{aligned}$$

where f'_n is the dimensionless equivalent of f_n . This form is convenient in that $C_{n_1}^2$ and $C_{n_2}^2$ now only appear in a ratio. It is not necessary to assume exact values, only a ratio of strengths at different altitudes in the two layer model.

3.5.3 SNR Equation The SNR may now be calculated using equations 3.47, 3.21, and 3.62 in equation 3.48. As a final simplification, let $\sigma' = \sigma L$. By using σ' in equation 3.62, the factor L^{-2} is common to the numerator and denominator of the SNR and is thereby eliminated. The equation for the SNR is

$$SNR = \quad (3.63)$$

$$\begin{aligned} & \left\{ 3.46 \left[1 + \frac{C_{n_2}^2}{C_{n_1}^2} \right]^{-1} \int_{-1}^1 du' \operatorname{tri}(u') f_6'(u') \right. \\ & \quad \left. + 3.46 \left[1 + \frac{C_{n_1}^2}{C_{n_2}^2} \right]^{-1} \int_{-1}^1 du' \operatorname{tri}(u') f_7'(u') \right\} \div \\ & \quad \left\{ 11.98 \left[\frac{C_{n_1}^2}{C_{n_2}^2} + \frac{C_{n_2}^2}{C_{n_1}^2} \right]^{-1} \int_{-1}^1 \int_{-1}^1 du' dv' \operatorname{tri}(u') \operatorname{tri}(v') \right. \\ & \quad \left. [f_1'(u', v') + f_2'(u', v') + f_3'(u', v')] \right. \\ & \quad + 6.92 \left(\frac{L}{r_0} \right)^{\frac{-5}{3}} \sigma'^2 \left[1 + \frac{C_{n_2}^2}{C_{n_1}^2} \right]^{-1} \int_{-1}^1 du \operatorname{tri}(u') f_4'(u') \\ & \quad + 6.92 \left(\frac{L}{r_0} \right)^{\frac{-5}{3}} \sigma'^2 \left[1 + \frac{C_{n_1}^2}{C_{n_2}^2} \right]^{-1} \int_{-1}^1 du' \operatorname{tri}(u') f_5'(u') \\ & \quad + \sigma'^4 \left(\frac{L}{r_0} \right)^{\frac{-10}{3}} \\ & \quad \left. - \left[3.46 \left[1 + \frac{C_{n_2}^2}{C_{n_1}^2} \right]^{-1} \int_{-1}^1 du' \operatorname{tri}(u') f_6'(u') \right. \right. \\ & \quad \left. \left. + 3.46 \left[1 + \frac{C_{n_1}^2}{C_{n_2}^2} \right]^{-1} \int_{-1}^1 du' \operatorname{tri}(u') f_7'(u') \right]^2 \right\}^{\frac{1}{2}} \end{aligned}$$

In the next chapter, some typical values are chosen for the geometry of figure 3.1 and the SNR is examined as several parameters are allowed to vary.

3.6 Conclusion

The correlation of wave front slope measurements has been related to C_n^2 by an integral expression involving a path weighting function. The characteristics of this function are examined in the next chapter. Also, a method to improve the path weighting function was discussed and an expression to calculate the signal-to-noise ratio of the correlation measurement was derived. These are also examined in the next chapter.

IV. Findings and Results

4.1 Introduction

This chapter presents the findings and results of this thesis research. The characteristics of the unmodified path weighting function are discussed first. It is shown that the shape of the weighting function must be modified to give it the characteristics of a sampling function. A method to improve the shape of the weighting function is presented, and the resolution possible with the improved function is calculated. Finally, assuming the turbulence is confined to two layers, the signal-to-noise ratio of the correlation measurement is calculated for a sample case.

4.2 Characteristics of the Path Weighting Function

In Chapter 3, the path weighting function was seen to be defined by the equation

$$w(z') = \tag{4.1}$$
$$-1.46k^2 L^{-\frac{1}{3}} \int_{-1}^1 du' \operatorname{tri}(u') \times$$
$$\left\{ 2 \left[\left(\frac{p}{L} \right)^2 + u'^2 \right]^{\frac{5}{6}} - \left[\left(\frac{p}{L} - 1 \right)^2 + u'^2 \right]^{\frac{5}{6}} - \left[\left(\frac{p}{L} + 1 \right)^2 + u'^2 \right]^{\frac{5}{6}} \right\}$$

where z' is point along the z axis, z_s is the height of the reference sources, Δx is the separation of the apertures, Δp is the separation of the reference sources, $k = \frac{2\pi}{\lambda}$, L is the dimension of the $L \times L$ apertures, and $p = \Delta p_x \frac{z'}{z_s} - \Delta x$ is the transverse separation of the ray paths. Recall that if $w(z')$ is to be useful as a sampling function, it should be at a maximum at the intersection point of the ray paths. The function should decay rapidly to zero away from the intersection point. A function exhibiting these characteristics could be used as a sampling function.

4.2.1 Unmodified Path Weighting Function The normalized path weighting function is plotted versus $\frac{p}{L}$ in figure 4.1. The data points used to create this plot were generated by the FORTRAN computer program NORMPATH contained in appendix A.1.

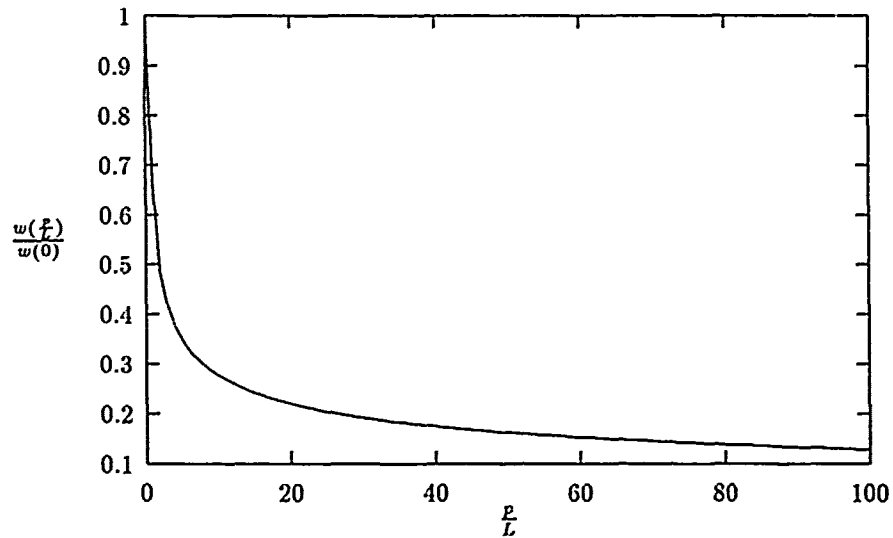


Figure 4.1. Normalized Path Weighting Function

When $\frac{p}{L} = 0$, the ray paths are at a point of intersection and the function is at a maximum. As $\frac{p}{L}$ increases, the ray paths diverge and the function falls off. Since the expression for the path weighting function was made dimensionless, the curve in figure 4.1 is the general shape for all values of L . For example, if $L = 1m$, the values on the horizontal axis range from 0 to 100m. If $L = 1cm$, the values range from 0 to 1m. A change in the value of L is therefore seen to control the decay time of the curve. As evidenced by figure 4.1, the path weighting function does exhibit the general required sampling characteristics. It has a maximum value at $\frac{p}{L} = 0$ and falls off as $\frac{p}{L}$ increases. However, the function does not fall off rapidly and never reaches a value of zero. The most rapid decay occurs when L is smallest, but the function still does not approach zero quickly enough. Therefore, the path weighting function must be modified to more closely approximate a sampling function, as shown in the next section.

4.2.2 Modified Path Weighting Function The method used to improve the shape of the path weighting function is to combine weighting functions generated by two apertures of sizes L_1 and L_2 . In particular, this should remove the common component of the average tilt and yield a function with a sharp falloff. By subtracting a weighting function generated by an aperture of size L_2 from that generated by an aperture of size L_1 , the common low spatial frequency components are removed. These low frequency components have a large correlation over large separations of the ray paths. The large correlation values associated with these low frequency components are what caused the previous results to be unacceptable. In effect, the subtraction is equivalent to a high pass filtering of the weighting function. A plot of the modified path weighting function is contained in figure 4.2 for three ratios of $\frac{L_1}{L_2}$. The data points used to create this plot were generated by the FORTRAN computer program MODPWF contained in appendix A.2.

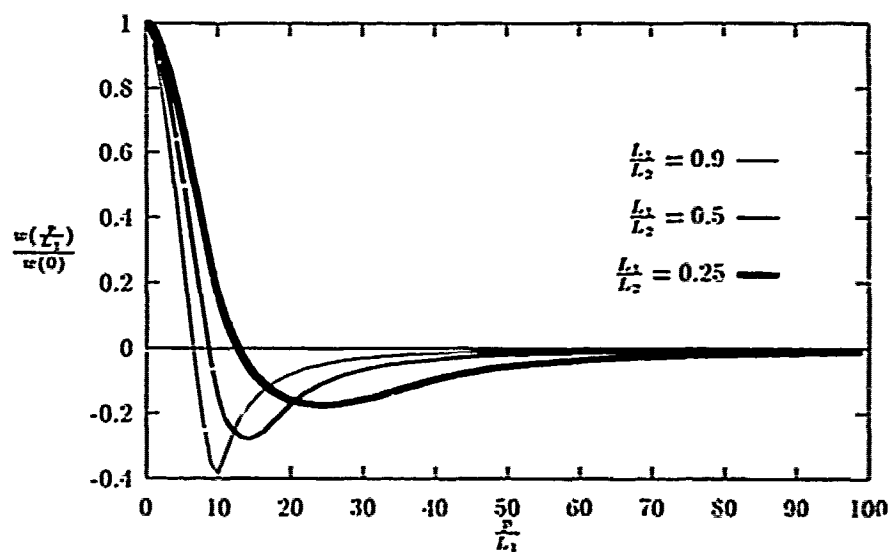


Figure 4.2. Modified Path Weighting Function

As with the normalized path weighting function plot, this method yields a family of curves. The horizontal spread is controlled by the size of L_1 and L_2 . As L_1 and L_2 get larger, the spread increases. This is because the low frequency components are correlated over a larger area. This action introduces a larger common tilt component. The rate of falloff to zero is controlled by the ratio $\frac{L_1}{L_2}$. As the ratio approaches 1, $w(\frac{p}{L_1})$ decays more rapidly. Therefore, the best sampling characteristics are exhibited by a curve that has small values for L_1 and L_2 and a ratio that approaches 1. If $L_1 = 1\text{cm}$ and $L_2 = 2\text{cm}$, the horizontal axis in figure 4.2 is scaled from 0 to 1m. For a ratio of 0.9, it is seen that the path weighting function goes to 0 when the transverse ray path separation is only 0.5 meters, which is very close to the intersection point. The plot shows that the modified path weighting function exhibits excellent sampling characteristics. The function falls off rapidly and stays at a zero value and could therefore be used to extract the value of C_n^2 from the correlation value.

4.3 Resolution of the Path Weighting Function

It has been shown that the modified path weighting function can be used as a sampling function. It now remains to determine the resolution of the function as it relates to the measurement geometry. The width of the function $w(z')$ may be interpreted as a measure of the vertical resolution. The narrower $w(z')$ is, the more accurate will be the value of C_n^2 that is calculated from $C_s(\vec{\Delta x})$. This may be directly related to the sifting property of the Dirac delta function.

To measure the vertical resolution, the method used by Welsh (18) is adopted. Recall that

$$p = \Delta p_r \frac{z'}{z_s} - \Delta x \quad (4.2)$$

At the intersection of the ray paths, $p = 0$ and the intersection altitude z_0 is given by

$$z_0 = \frac{\Delta x z_s}{\Delta p_r} \quad (4.3)$$

Let a measure of the width of $w(z')$ be given by the point $p = p'$ where, for example, p' is the e^{-1} point of $w(\frac{p}{L})$. Designate the altitude corresponding to this point as $z_{p'}$. Solving for $z_{p'}$:

$$z_{p'} = \frac{(p' + \Delta x) z_s}{\Delta p_x} \quad (4.4)$$

The width of $w(z)$, with respect to z , is

$$\Delta z = z_0 - z_p = \frac{p' z_s}{\Delta p_x} \quad (4.5)$$

Let θ designate the angle between ray paths. As seen from figure 3.1, this is also the angular separation of the point sources. θ may be expressed as

$$\frac{\theta}{2} = \arctan \left(\frac{\Delta p_x}{2z_s} \right) \quad (4.6)$$

Solving for Δp_x ,

$$\Delta p_x = 2z_s \tan\left(\frac{\theta}{2}\right) \quad (4.7)$$

Using equation 4.7, equation 4.5 may be expressed as

$$\Delta z = \frac{p'}{2 \tan(\frac{\theta}{2})} \quad (4.8)$$

As an example, referring to figure 4.2, for $L_1 = 1cm$, $L_2 = 2cm$, and $\frac{L_1}{L_2} = 0.5$, it is seen that the width of $w(\frac{p}{L})$ is approximately $p = 0.8m$. Using this value for p' , vertical resolution is plotted as a function of θ in figure 4.3.

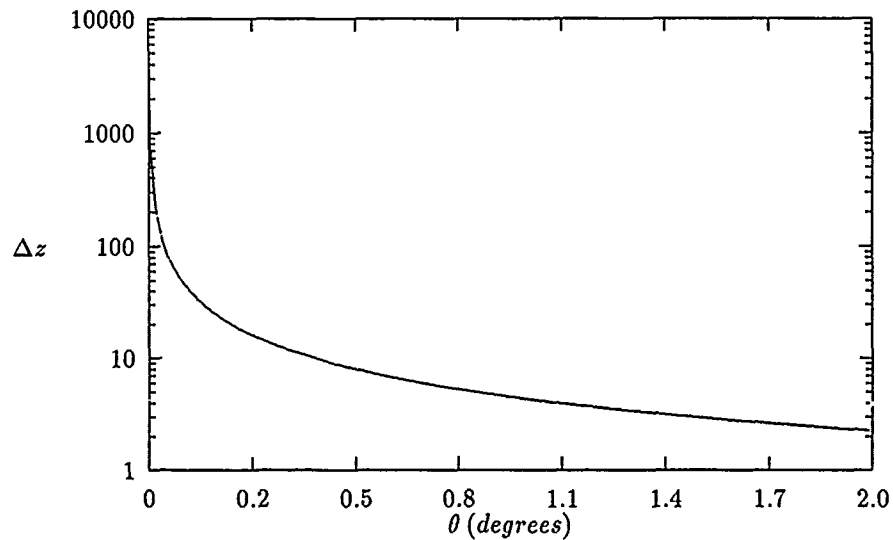


Figure 4.3. Vertical Resolution

The plot clearly shows that resolution is related to separation of the point sources. For example, if 10 meter resolution is required, θ must be approximately 0.4 degrees. In general, resolution increases as source separation increases.

4.4 Signal-to-Noise Ratio of the Correlation Measurement

In order to quantify the usefulness of the methods presented in this thesis, the SNR of the correlation measurement is calculated. The reader is referred to Chapter 3 for the derivation and defining equations. It is important to note the SNR analysis is valid for the case of the unmodified path weighting function only. While this provides a good initial look at the problem, the analysis should be extended in the future.

To evaluate the SNR for a typical case, it was necessary to choose values for several parameters. The reader will recall that $\sigma'^2 \times (\frac{L}{r_0})^{\frac{2}{3}}$ was a parameter in the SNR equation that characterizes the noise in the process. This parameter will be allowed to vary to see how noise effects the SNR. The structure constant ratio $\frac{C_{n_2}^2}{C_{n_1}^2} = 2.5$ was used based on the data in figure 2.1. Assuming the turbulence is confined to two layers, the peaks of the curve at 1 and 10km are chosen. The approach taken is to divide the area under the curve into two sections and assume it exists as delta functions at the peak values. The area under the curve from 1 to 10km is calculated and assumed to exist as a delta function at 1km. In the same fashion, the area from 10 to 20km is calculated and assumed to exist as a delta function at 20km. The resulting ratio is 2.5.

The reference sources are assumed to be laser guidestars at an altitude of $z_s = 100km$. Guidestar separation, Δp_r , is 1km. The data points used to create the plots in the following subsections were generated by the FORTRAN computer program SNR in appendix A.3.

4.4.1 *SNR as a Function of Noise* Welsh and Gardner (19:1919) provide an expression for the tilt measurement error (noise) as follows:

$$\sigma = \frac{0.86\pi\eta}{N^{\frac{1}{2}}r_0} \quad L > r_0 \quad (4.9)$$

where η is a parameter used to account for imperfections in the detector array and N is the total subaperture photon count. $\eta = 1.5$ is used as a typical value.

Using equation 4.9 and recalling $\sigma' = \sigma L$, it is possible to relate σ'^2 to the photon count for the values used in the sample case. The resulting equation is

$$\frac{N}{(\frac{L}{r_0})^{\frac{1}{3}}} = \frac{(0.86\pi\eta)^2}{\sigma'^2(\frac{L}{r_0})^{\frac{2}{3}}} \quad (4.10)$$

where the parameter $\sigma'^2(\frac{L}{r_0})^{\frac{2}{3}}$ has been introduced to coincide with the terms in the SNR equation in Chapter 3. The photon count may now be related to the SNR using equation 4.10. This relationship is plotted in figure 4.4.

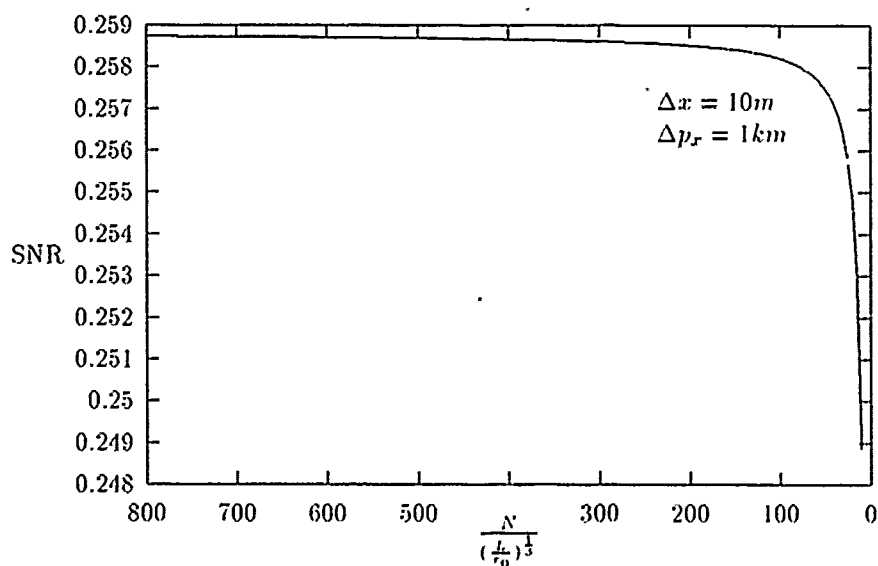


Figure 4.4. SNR as a Function of Photon Count

The plot shows that a photon count of greater than 200 produces an SNR very close to the noiseless value. Assuming that bright guidestars are used (i.e. created with sufficient power), photon noise should not be a concern. The remainder of the SNR analysis will therefore assume a noiseless system (i.e. $\sigma' = 0$).

4.4.2 SNR as a Function of Ray Path Separation In this subsection, the effect on the SNR of changing the ray path separation is investigated. There are two ways to change the path separation; by changing the separation of the subapertures or by changing the separation of the point sources. In figure 4.5, the subaperture separation, Δx , is allowed to vary. Recall that z_1 is the height of the first turbulence layer, z_2 is the height of the second turbulence layer, z_s is the guidestar height, and Δp_x is the guidestar separation. The separation of ray paths is given by $\Delta p_x \frac{z'}{z_s} - \Delta x$. Therefore, the two points of interest on the plot are when $\Delta x = \Delta p_x \frac{z_1}{z_s}$ and $\Delta x = \Delta p_x \frac{z_2}{z_s}$. These points correspond to a path intersection point for each turbulence layer and occur at $\Delta x = 10$ and $\Delta x = 100$. In figure 4.6, the guidestar separation, Δp_x is allowed to vary. The corresponding intersection points for the turbulence layers are at $\Delta p_x = 100m$ and $\Delta p_x = 1km$.

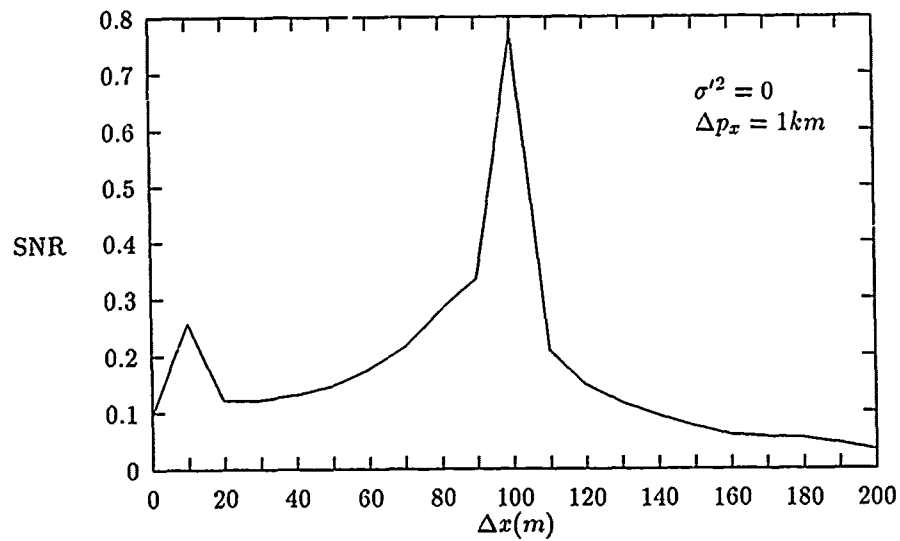


Figure 4.5. SNR as a Function of Subaperture Separation

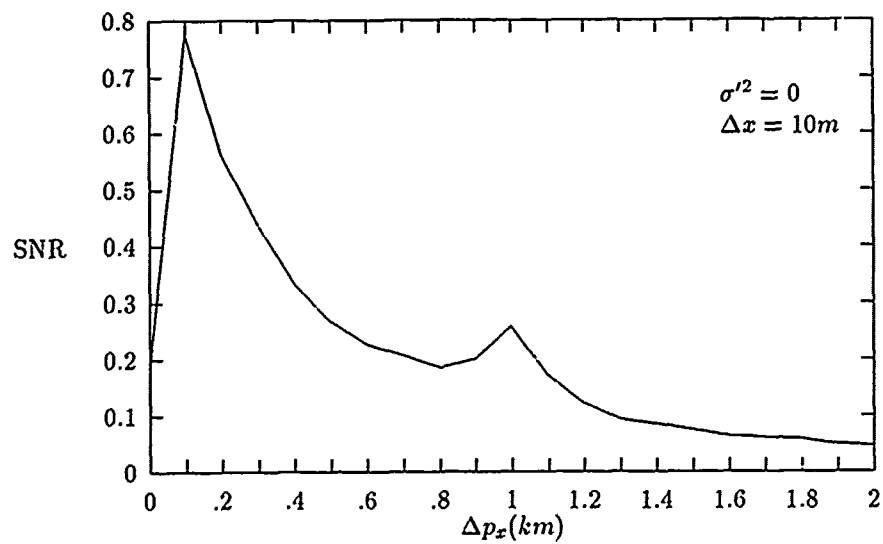


Figure 4.6. SNR as a Function of Source Separation

As seen from the plots, the SNR reaches two maximum values. While the plots appear to be in reverse order, it is important to realize that the SNR values are consistent between the two plots. For example, the value of 0.259 at $\Delta x = 10m$ and $\Delta p_z = 1km$ is consistent between the two plots. This becomes clear when one considers what is happening when either the source or subaperture separation is increased. The net effect is to change ray path separation, however, the change is initiated at opposite ends and this causes the plots to appear reversed.

The difference in the height of the peaks in the turbulence layers may be directly related to the strength of the turbulence at the layers. The stronger turbulence is causing a higher correlation value and hence a larger SNR. It may be assumed that it will be easier to detect stronger turbulence values with this method.

The variation in the plot of the SNR indicates that different combinations of source and subaperture separations yield different values of the SNR. Depending on the application and physical limitations of an experiment (i.e. physical space available to change the separation of the wave front sensors), one may adjust the interrelationship for an optimum SNR.

4.4.3 Improvement of the SNR The SNR plots in the previous section did not exceed a value of 1. For the method to be useful, it is necessary to consider how the SNR may be increased. The reader will recall an initial assumption in Chapter 3 restricted the wave front sensors to a single subaperture. If sensors with multiple subapertures are used, an array of correlation values will be obtained. This is done by pairing all possible combinations of the subapertures, each pair being separated by Δx . Using an array of n values should improve the SNR by a factor of n . This action should raise the SNR to a level suitable for detection.

4.5 Obtaining a Vertical Profile

As was seen in the previous section, changing the subaperture separation moves the path intersection point vertically. This feature may be exploited to obtain a vertical profile of C_n^2 . If sensors with multiple subapertures are used, it is possible use many different values of Δx . Pairing all possible combinations of subapertures separated by all values of Δx will result in an array of correlation values that correspond to different intersection altitudes. These values may be exploited to extract the value of C_n^2 at the different altitudes.

4.6 Conclusion

It has been shown that, using the subtraction method, the path weighting function can be modified to approximate a sampling function. C_s can be directly related to C_n^2 by the modified function. The resolution plot indicates that source separation determines the vertical resolution. As source separation increases, vertical resolution increases. The SNR calculations for the sample case show that wave front sensors with multiple subapertures will be necessary. If multiple values are obtained to raise the SNR, it will be possible to extract the value of C_n^2 from the value of C_s . Using multiple subapertures also allows one to obtain a vertical profile.

V. Conclusions and Recommendations

5.1 Overview

This chapter contains the conclusions drawn from this research. It also contains the authors recommendations for further study.

5.2 Conclusions

This research has shown that the spatial correlation of wave front slopes may be used to calculate the value of the atmospheric structure constant. The correlation process yields an integral expression relating C_n^2 to the correlation value by means of a path weighting function. It is possible to shape the weighting function into a sampling function and to use the sifting property of the sampling function to directly relate C_n^2 to the correlation measurement.

It is difficult to compare the accuracy of this method to other methods. Typically, other methods of calculating C_n^2 are experimentally implemented and the results of the experiment are compared against known values of C_n^2 . That has not been done yet with this research. However, based on the sample SNR calculation for two-layer turbulence, it is anticipated this method will yield accurate results. Full-scale modeling and testing should prove this assertion to be true.

5.3 Recommendations

The following suggestions for further study are made.

1. The SNR analysis should be extended beyond the assumption that the turbulence is confined to two layers. Increasing the number of turbulent layers will more closely approximate a real-life situation.
2. The SNR analysis should be done for the case of the modified path weighting function.
3. Using an accepted model for atmospheric turbulence, this research method should be computer modeled. The spatial correlation of wave front phase slopes should be calculated for the modeled scenario and compared to known results to determine the accuracy of this method.
4. This method should be experimentally verified and the results should be compared to those obtained by other measurement methods.

5.4 *Summary*

The spatial correlation of wave front slopes from two point sources theoretically yields a value for C_n^2 . Experimental verification of the method will allow it to become another tool to calculate the magnitude of atmospheric turbulence.

Appendix A. *Computer Programs*

This appendix contains the FORTRAN computer code used to obtain the plots in Chapter 4 of this thesis. The code was written by the author with the exception of QSIMP, TRAPZD, and INTEG2D. These were adapted from the book Numerical Recipes: The Art of Scientific Computing by William H. Press, Brian P. Flannery, Saul A. Teukolsky, and William T. Vetterling published by Cambridge University Press, New York, 1986, pages 110-130.

A.1 *Program NORMPATH*

```
PROGRAM NORMPATH
*
*   This program computes the values for the
*   normalized path weighting function.
*
EXTERNAL WTFUNC
COMMON /PARAMS/P,L
REAL P,PPRIME,L,NORM,STEP
INTEGER I
100  FORMAT (F10.3)
    OPEN(UNIT=10, NAME='PROG1.DAT', STATUS='NEW')
*
    READ(5,100) L
    READ(5,100) STEP
    P=0.
*
    CALL QSIMP(WTFUNC,-1,1,S)
    NORM=S*(L**(-1./3.))
    DO 110 I=0,100
        PPRIME=P/L
        CALL QSIMP(WTFUNC,-1,1,S)
        S=(S/NORM)*(L**(-1./3.))
        WRITE(10,100) PPRIME,S
        P=P+STEP
110  CONTINUE
*
    CLOSE(UNIT=10)
    STOP
    END
*****
REAL FUNCTION WTFUNC(X)
```

```

COMMON /PARAMS/P,L
REAL P,L
WTFUNC=- (1.-ABS(X))* (
C      2.*(((P/L)**2.+(X)**2.)*(5./6.))-
C      (((P/L)-1.)*(5./6.))-
C      (((P/L)+1.)*(5./6.))
C      )
RETURN
END

*****
SUBROUTINE TRAPZD(FUNC,A,B,S,N)
IF (N.EQ.1) THEN
  S=0.5*(B-A)*(FUNC(A)+FUNC(B))
  IT=1
ELSE
  TNM=IT
  DEL=(B-A)/TNM
  X=A+0.5*DEL
  SUM=0.
  DO 200 J=1,IT
    SUM=SUM+FUNC(X)
    X=X+DEL
200  CONTINUE
  S=0.5*(S+(B-A)*SUM/TNM)
  IT=2*IT
ENDIF
RETURN
END

*****
SUBROUTINE QSIMP(FUNC,A,B,S)
PARAMETER (EPS=1.E-5, JMAX=20)
OST=-1.E30
OS= -1.E30
DO 300 J=1,JMAX
  CALL TRAPZD(FUNC,A,B,ST,J)
  S=(4.*ST-OST)/3.
  IF (ABS(S-OS).LT.EPS*ABS(OS)) RETURN
  OS=S
  OST=ST
300  CONTINUE
  PAUSE 'Too many steps.'
END

```

A.2 Program MODPWF

```
PROGRAM MODPWF
*
*   This program subtracts a weighting function
*   for an aperture of size L2 from a weighting
*   function for an aperture of size L1.
*   The values are normalized for a maximum of 1.
*
EXTERNAL WTFUNCL1,WTFUNCL2
COMMON /PARAMS/P,L1,L2,RATIO
REAL P,PPRIME,L,L1,L2,RATIO,NORM,STEP
INTEGER I
100  FORMAT (F10.3)
    OPEN(UNIT=10, NAME='PROG1.DAT', STATUS='NEW')
*
    P=0.
    READ(5,100) L1
    READ(5,100) RATIO
    READ(5,100) STEP
    L2=L1/RATIO
*
    DO 110 I=0,100
        L=L1
        CALL QSIMP(WTFUNCL1,-1.,1.,SA)
        SA=SA*(L1**(-1./3.))
        L=L2
        CALL QSIMP(WTFUNCL2,-1.,1.,SB)
        SB=SB*(L2**(-1./3.))
        S=SA-SB
        IF (I .EQ. 0) THEN
            NORM=S
        ENDIF
        S=S/NORM
        PPRIME=P/L1
        WRITE(10,100) PPRIME,S
        P=P+STEP
110  CONTINUE
*
    CLOSE(UNIT=10)
    STOP
    END
*****
REAL FUNCTION WTFUNCL1(X)
COMMON /PARAMS/P,L1,L2,RATIO
```

```

      REAL P,L1,L2,RATIO
      WTFUNCL1=- (1.-ABS(X))*(
C          2.*((P/L1)**2.+(X)**2.)*(5./6.))-
C          ((P/L1-1)**2.+(X)**2.)*(5./6.)-
C          ((P/L1+1)**2.+(X)**2.)*(5./6.)
C      )
      RETURN
      END
*****
      REAL FUNCTION WTFUNCL2(X)
      COMMON /PARAMS/P,L1,L2,RATIO
      REAL P,L1,L2,RATIO
      WTFUNCL2=- (1.-ABS(X))*(
C          2.*((P/L2)**2.+(X)**2.)*(5./6.))-
C          ((P/L2-1)**2.+(X)**2.)*(5./6.)-
C          ((P/L2+1)**2.+(X)**2.)*(5./6.)
C      )
      RETURN
      END
*****
      SUBROUTINE TRAPZD(FUNC,A,B,S,N)
      IF (N.EQ.1) THEN
          S=0.5*(B-A)*(FUNC(A)+FUNC(B))
          IT=1
      ELSE
          TNM=IT
          DEL=(B-A)/TNM
          X=A+0.5*DEL
          SUM=0.
          DO 200 J=1,IT
              SUM=SUM+FUNC(X)
              X=X+DEL
200      CONTINUE
          S=0.5*(S+(B-A)*SUM/TNM)
          IT=2*IT
      ENDIF
      RETURN
      END
*****
      SUBROUTINE QSIMP(FUNC,A,B,S)
      PARAMETER (EPS=1.E-5, JMAX=20)
      OST=-1.E30
      OS= -1.E30
      DO 300 J=1,JMAX
          CALL TRAPZD(FUNC,A,B,ST,J)

```

```
S=(4.*ST-OST)/3.  
IF (ABS(S-OS).LT.EPS*ABS(OS)) RETURN  
OS=S  
OST=ST  
300 CONTINUE  
PAUSE 'Too many steps.'  
END
```

A.3 Program SNR

```
PROGRAM SNR
*
*   This program computes the mean and variance
*   of the correlation of wave front phase slopes.
*   It then calculates the signal-to-noise ratio
*   from the relationship  $SNR=MEAN/SQRT(VAR)$ .
*
EXTERNAL WTFUNCA1,WTFUNCA2,WTFUNCB
EXTERNAL WTFUNCC,WTFUNCD,WTFUNCE
EXTERNAL G,H
COMMON /PARAMS/P1,P2,P3,P4
COMMON/FLGS/FLAG
REAL P1,P2,P3,P4
REAL SA,SB,SC,SD,SE,S
REAL CA,CB,CC,CD,CE
REAL L_RO,CN21,DELTAX,DEL_PX,NOIVAR
REAL MEAN,VAR,SNR
INTEGER I,FLAG
*
100  FORMAT (F10.3)
    OPEN(UNIT=10, NAME='PROG1.DAT', STATUS='NEW')
*
    L_RO=10.
    CN21=2.5
    DELTAX=10.
    DEL_PX=1000.
    P1=DEL_PX/100.
    P2=DEL_PX/10.
    P3=(P1-DELTAX)
    P4=(P2-DELTAX)
    NOIVAR=0.
*
    DO 110 I=0,100
        CA=11.98*(1/(CN21+1/CN21))
        CB=6.92*(L_RO**(-5./3.))*
C      (1/(1+CN21))*NOIVAR
        CC=6.92*(L_RO**(-5./3.))*
C      (1/(1+1/CN21))*NOIVAR
        CD=-3.46*(1/(1+CN21))
        CE=-3.46*(1/(1+1/CN21))
        FLAG=1
        CALL INTEG2D(-1.,1.,S)
        SA1=S
```

```

        FLAG=2
        CALL INTEG2D(-1.,1.,S)
        SA2=S
        CALL QSIMP(WTFUNCB,-1.,1.,SB)
        CALL QSIMP(WTFUNCC,-1.,1.,SC)
        CALL QSIMP(WTFUNCD,-1.,1.,SD)
        CALL QSIMP(WTFUNCE,-1.,1.,SE)
        MEAN=ABS(CD*SD+CE*SE)
        VAR=(CA*(SA1+SA2))+(CB*SB)+(CC*SC)+
C      (NOIVAR**2.*L_RO**(-10./3.)-(MEAN**2.))
        SNR=MEAN/SQRT(VAR)
        WRITE(10,100) SNR

*
* Depending on the parameter being modified to see
* the effect on the SNR, code must be added here.
* For example, if the effect of noise on the SNR is
* the quantity of interest, NOIVAR=NOIVAR+1. may
* be used.
*
110    CONTINUE
*
        CLOSE(UNIT=10)
        STOP
        END

*****
        SUBROUTINE INTEG2D(X1,X2,S)
        EXTERNAL H
        COMMON /PARAMS/P1,P2,P3,P4
        REAL P1,P2,P3,P4
        CALL QSIMPX(H,-1.,1.,S)
        RETURN
        END

*****
        REAL FUNCTION H(XX)
        EXTERNAL G
        COMMON/XY/X,Y
        COMMON /PARAMS/P1,P2,P3,P4
        REAL P1,P2,P3,P4
        X=XX
        CALL QSIMPY(G,-1.,1.,S)
        H=S
        RETURN
        END

*****
        REAL FUNCTION G(YY)

```

```

EXTERNAL WTFUNCA1,WTFUNCA2
COMMON/XY/X,Y
COMMON/PARAMS/P1,P2,P3,P4
COMMON/FLGS/FLAG
INTEGER FLAG
REAL P1,P2,P3,P4
Y=YY
      IF (FLAG .EQ. 1) THEN
            G=WTFUNCA1(X,Y)
      ELSE
            G=WTFUNCA2(X,Y)
      ENDIF
RETURN
END
*****
      REAL FUNCTION WTFUNCA1(X,Y)
      COMMON /PARAMS/P1,P2,P3,P4
      REAL P1,P2,P3,P4
      WTFUNCA1=(1.-ABS(X))*(1.-ABS(Y))*(
C      4.*(P1**2.+X**2.)*(5./6.)*
C      (P1**2.+Y**2.)*(5./6.)+
C      ((P1+1.）**2.+X**2.)*(5./6.)*
C      ((P1+1.）**2.+Y**2.)*(5./6.)+
C      ((P1-1.）**2.+X**2.)*(5./6.)*
C      ((P1+1.）**2.+Y**2.)*(5./6.)+
C      ((P1+1.）**2.+X**2.)*(5./6.)*
C      ((P1-1.）**2.+Y**2.)*(5./6.)+
C      ((P1-1.）**2.+X**2.)*(5./6.)*
C      ((P1-1.）**2.+Y**2.)*(5./6.)*
C      2.*((P1+1.）**2.+X**2.)*(5./6.)*
C      ((P1)**2.+Y**2.)*(5./6.)*
C      2.*((P1-1.）**2.+X**2.)*(5./6.)*
C      ((P1)**2.+Y**2.)*(5./6.)*
C      2.*((P1)**2.+X**2.)*(5./6.)*
C      ((P1-1.）**2.+Y**2.)*(5./6.)*
C      2.*((P1)**2.+X**2.)*(5./6.)*
C      ((P1+1.）**2.+Y**2.)*(5./6.)*
C      4.*(P1**2.+X**2.)*(5./6.)*
C      (P2**2.+Y**2.)*(5./6.)*
C      ((P1+1.）**2.+X**2.)*(5./6.)*
C      ((P2+1.）**2.+Y**2.)*(5./6.)*
C      ((P1-1.）**2.+X**2.)*(5./6.)*
C      ((P2+1.）**2.+Y**2.)*(5./6.)*
C      ((P1+1.）**2.+X**2.)*(5./6.)*
C      ((P2-1.）**2.+Y**2.)*(5./6.)*

```

C $((P1-1.)^{**2}+X^{**2.})^{**}(5./6.)*$
 C $((P2-1.)^{**2}+Y^{**2.})^{**}(5./6.)-$
 C $2.*((P1+1.)^{**2}+X^{**2.})^{**}(5./6.)*$
 C $((P2)^{**2}+Y^{**2.})^{**}(5./6.)-$
 C $2.*((P1-1.)^{**2}+X^{**2.})^{**}(5./6.)*$
 C $((P2)^{**2}+Y^{**2.})^{**}(5./6.)-$
 C $2.*((P1)^{**2}+X^{**2.})^{**}(5./6.)*$
 C $((P2-1.)^{**2}+Y^{**2.})^{**}(5./6.)-$
 C $2.*((P1)^{**2}+X^{**2.})^{**}(5./6.)*$
 C $((P2+1.)^{**2}+Y^{**2.})^{**}(5./6.)+$
 C $4.*(P2^{**2}+X^{**2.})^{**}(5./6.)*$
 C $(P1^{**2}+Y^{**2.})^{**}(5./6.)+$
 C $((P2+1.)^{**2}+X^{**2.})^{**}(5./6.)*$
 C $((P1+1.)^{**2}+Y^{**2.})^{**}(5./6.)+$
 C $((P2-1.)^{**2}+X^{**2.})^{**}(5./6.)*$
 C $((P1+1.)^{**2}+Y^{**2.})^{**}(5./6.)+$
 C $((P2+1.)^{**2}+X^{**2.})^{**}(5./6.)*$
 C $((P1-1.)^{**2}+Y^{**2.})^{**}(5./6.)+$
 C $((P2-1.)^{**2}+X^{**2.})^{**}(5./6.)*$
 C $((P1-1.)^{**2}+Y^{**2.})^{**}(5./6.)-$
 C $2.*((P2+1.)^{**2}+X^{**2.})^{**}(5./6.)*$
 C $((P1)^{**2}+Y^{**2.})^{**}(5./6.)-$
 C $2.*((P2-1.)^{**2}+X^{**2.})^{**}(5./6.)*$
 C $((P1)^{**2}+Y^{**2.})^{**}(5./6.)-$
 C $2.*((P2)^{**2}+X^{**2.})^{**}(5./6.)*$
 C $((P1-1.)^{**2}+Y^{**2.})^{**}(5./6.)-$
 C $2.*((P2)^{**2}+X^{**2.})^{**}(5./6.)*$
 C $((P1+1.)^{**2}+Y^{**2.})^{**}(5./6.)+$
 C $4.*(P2^{**2}+X^{**2.})^{**}(5./6.)*$
 C $(P2^{**2}+Y^{**2.})^{**}(5./6.)+$
 C $((P2+1.)^{**2}+X^{**2.})^{**}(5./6.)*$
 C $((P2+1.)^{**2}+Y^{**2.})^{**}(5./6.)+$
 C $((P2-1.)^{**2}+X^{**2.})^{**}(5./6.)*$
 C $((P2+1.)^{**2}+Y^{**2.})^{**}(5./6.)+$
 C $((P2+1.)^{**2}+X^{**2.})^{**}(5./6.)*$
 C $((P2-1.)^{**2}+Y^{**2.})^{**}(5./6.)+$
 C $((P2-1.)^{**2}+X^{**2.})^{**}(5./6.)*$
 C $((P2-1.)^{**2}+Y^{**2.})^{**}(5./6.)-$
 C $2.*((P2+1.)^{**2}+X^{**2.})^{**}(5./6.)*$
 C $((P2)^{**2}+Y^{**2.})^{**}(5./6.)-$
 C $2.*((P2-1.)^{**2}+X^{**2.})^{**}(5./6.)*$
 C $((P2)^{**2}+Y^{**2.})^{**}(5./6.)-$
 C $2.*((P2)^{**2}+X^{**2.})^{**}(5./6.)*$
 C $((P2-1.)^{**2}+Y^{**2.})^{**}(5./6.)-$
 C $2.*((P2)^{**2}+X^{**2.})^{**}(5./6.)*$

```

C  ((P2+1.)**2.+Y**2.)**(5./6.)
C  )
RETURN
END
*****
REAL FUNCTION WTFUNCA2(X,Y)
COMMON /PARAMS/P1,P2,P3,P4
REAL P1,P2,P3,P4
WTFUNCA2=(1.-ABS(X))*(1.-ABS(Y))*2*(
C  4.*(P3**2.+X**2.)**(5./6.)*
C  (P3**2.+Y**2.)**(5./6.)+
C  ((P3+1.)**2.+X**2.)**(5./6.)*
C  ((P3+1.)**2.+Y**2.)**(5./6.)+
C  ((P3-1.)**2.+X**2.)**(5./6.)*
C  ((P3+1.)**2.+Y**2.)**(5./6.)+
C  ((P3+1.)**2.+X**2.)**(5./6.)*
C  ((P3-1.)**2.+Y**2.)**(5./6.)+
C  ((P3-1.)**2.+X**2.)**(5./6.)*
C  ((P3-1.)**2.+Y**2.)**(5./6.)-
C  2.*((P3+1.)**2.+X**2.)**(5./6.)*
C  ((P3)**2.+Y**2.)**(5./6.)-
C  2.*((P3-1.)**2.+X**2.)**(5./6.)*
C  ((P3)**2.+Y**2.)**(5./6.)-
C  2.*((P3)**2.+X**2.)**(5./6.)*
C  ((P3-1.)**2.+Y**2.)**(5./6.)-
C  2.*((P3)**2.+X**2.)**(5./6.)*
C  ((P3+1.)**2.+Y**2.)**(5./6.)+
C  4.*(P3**2.+X**2.)**(5./6.)*
C  (P4**2.+Y**2.)**(5./6.)+
C  ((P3+1.)**2.+X**2.)**(5./6.)*
C  ((P4+1.)**2.+Y**2.)**(5./6.)+
C  ((P3-1.)**2.+X**2.)**(5./6.)*
C  ((P4+1.)**2.+Y**2.)**(5./6.)+
C  ((P3+1.)**2.+X**2.)**(5./6.)*
C  ((P4-1.)**2.+Y**2.)**(5./6.)+
C  ((P3-1.)**2.+X**2.)**(5./6.)*
C  ((P4-1.)**2.+Y**2.)**(5./6.)-
C  2.*((P3+1.)**2.+X**2.)**(5./6.)*
C  ((P4)**2.+Y**2.)**(5./6.)-
C  2.*((P3-1.)**2.+X**2.)**(5./6.)*
C  ((P4)**2.+Y**2.)**(5./6.)-
C  2.*((P3)**2.+X**2.)**(5./6.)*
C  ((P4-1.)**2.+Y**2.)**(5./6.)-
C  2.*((P3)**2.+X**2.)**(5./6.)*
C  ((P4+1.)**2.+Y**2.)**(5./6.)+

```

```

C  4.*(P4**2.+X**2.)*(5./6.)*
C  (P3**2.+Y**2.)*(5./6.)+
C  ((P4+1.)*2.+X**2.)*(5./6.)*
C  ((P3+1.)*2.+Y**2.)*(5./6.)+
C  ((P4-1.)*2.+X**2.)*(5./6.)*
C  ((P3+1.)*2.+Y**2.)*(5./6.)+
C  ((P4+1.)*2.+X**2.)*(5./6.)*
C  ((P3-1.)*2.+Y**2.)*(5./6.)+
C  ((P4-1.)*2.+X**2.)*(5./6.)*
C  ((P3-1.)*2.+Y**2.)*(5./6.)-
C  2.*((P4+1.)*2.+X**2.)*(5./6.)*
C  ((P3)**2.+Y**2.)*(5./6.)-
C  2.*((P4-1.)*2.+X**2.)*(5./6.)*
C  ((P3)**2.+Y**2.)*(5./6.)-
C  2.*((P4)**2.+X**2.)*(5./6.)*
C  ((P3-1.)*2.+Y**2.)*(5./6.)-
C  2.*((P4)**2.+X**2.)*(5./6.)*
C  ((P3+1.)*2.+Y**2.)*(5./6.)+
C  4.*(P4**2.+X**2.)*(5./6.)*
C  (P4**2.+Y**2.)*(5./6.)+
C  ((P4+1.)*2.+X**2.)*(5./6.)*
C  ((P4+1.)*2.+Y**2.)*(5./6.)+
C  ((P4-1.)*2.+X**2.)*(5./6.)*
C  ((P4+1.)*2.+Y**2.)*(5./6.)+
C  ((P4+1.)*2.+X**2.)*(5./6.)*
C  ((P4-1.)*2.+Y**2.)*(5./6.)+
C  ((P4-1.)*2.+X**2.)*(5./6.)*
C  ((P4-1.)*2.+Y**2.)*(5./6.)-
C  2.*((P4+1.)*2.+X**2.)*(5./6.)*
C  ((P4)**2.+Y**2.)*(5./6.)-
C  2.*((P4-1.)*2.+X**2.)*(5./6.)*
C  ((P4)**2.+Y**2.)*(5./6.)-
C  2.*((P4)**2.+X**2.)*(5./6.)*
C  ((P4-1.)*2.+Y**2.)*(5./6.)-
C  2.*((P4)**2.+X**2.)*(5./6.)*
C  ((P4+1.)*2.+Y**2.)*(5./6.)
C  )

```

RETURN

END

REAL FUNCTION WTFUNCB(X)

COMMON /PARAMS/P3,P2,P3,P4

REAL P1,P2,P3,P4

WTFUNCB=-(1.-ABS(X))*(

```

C      2.*(P1**2.+X**2.)*(5./6.)-

```

```

C      ((P1-1.):**2.+X**2.):**5./6.)-
C      ((P1+1.):**2.+X**2.):**5./6.)
C      )
      RETURN
      END
*****
      REAL FUNCTION WTFUNCC(X)
      COMMON /PARAMS/P1,P2,P3,P4
      REAL P1,P2,P3,P4
      WTFUNCC=-(1.-ABS(X))*(
C      2.*(P2**2.+X**2.):**5./6.)-
C      ((P2-1.):**2.+X**2.):**5./6.)-
C      ((P2+1.):**2.+X**2.):**5./6.)
C      )
      RETURN
      END
*****
      REAL FUNCTION WTFUNCD(X)
      COMMON /PARAMS/P1,P2,P3,P4
      REAL P1,P2,P3,P4
      WTFUNCD=-(1.-ABS(X))*(
C      2.*((P3)**2.+X**2.):**5./6.)-
C      ((P3-1.):**2.+X**2.):**5./6.)-
C      ((P3+1.):**2.+X**2.):**5./6.)
C      )
      RETURN
      END
*****
      REAL FUNCTION WTFUNCE(X)
      COMMON /PARAMS/P1,P2,P3,P4
      REAL P1,P2,P3,P4
      WTFUNCE=-(1.-ABS(X))*(
C      2.*((P4)**2.+X**2.):**5./6.)-
C      ((P4-1.):**2.+X**2.):**5./6.)-
C      ((P4+1.):**2.+X**2.):**5./6.)
C      )
      RETURN
      END
*****
      SUBROUTINE TRAPZD(FUNC,A,B,S,N)
      IF (N.EQ.1) THEN
        S=0.5*(B-A)*(FUNC(A)+FUNC(B))
        IT=1
      ELSE
        TNM=IT

```

```

        DEL=(B-A)/TNM
        X=A+0.5*DEL
        SUM=0.
        DO 200 J=1,IT
            SUM=SUM+FUNC(X)
            X=X+DEL
200      CONTINUE
        S=0.5*(S+(B-A)*SUM/TNM)
        IT=2*IT
    ENDIF
    RETURN
    END
*****
    SUBROUTINE QSIMP(FUNC,A,B,S)
    PARAMETER (EPS=1.E-5, JMAX=20)
    OST=-1.E30
    OS= -1.E30
    DO 300 J=1,JMAX
        CALL TRAPZD(FUNC,A,B,ST,J)
        S=(4.*ST-OST)/3.
        IF (ABS(S-OS).LT.EPS*ABS(OS)) RETURN
        OS=S
        OST=ST
300    CONTINUE
    PAUSE 'Too many steps.'
    END
*****
    SUBROUTINE TRAPZDX(FUNC,A,B,S,N)
    IF (N.EQ.1) THEN
        S=0.5*(B-A)*(FUNC(A)+FUNC(B))
        IT=1
    ELSE
        TNM=IT
        DEL=(B-A)/TNM
        X=A+0.5*DEL
        SUM=0.
        DO 200 J=1,IT
            SUM=SUM+FUNC(X)
            X=X+DEL
200    CONTINUE
        S=0.5*(S+(B-A)*SUM/TNM)
        IT=2*IT
    ENDIF
    RETURN
    END

```

```

SUBROUTINE QSIMPX(FUNC,A,B,S)
  PARAMETER (EPS=1.E-5, JMAX=20)
  OST=-1.E30
  OS= -1.E30
  DO 300 J=1,JMAX
    CALL TRAPZDX(FUNC,A,B,ST,J)
    S=(4.*ST-OST)/3.
    IF (ABS(S-OS).LT.EPS*ABS(OS)) RETURN
    OS=S
    OST=ST
300  CONTINUE
  PAUSE 'Too many steps.'
  END

```

```

SUBROUTINE TRAPZDY(FUNC,A,B,S,N)
  IF (N.EQ.1) THEN
    S=0.5*(B-A)*(FUNC(A)+FUNC(B))
    IT=1
  ELSE
    TNM=IT
    DEL=(B-A)/TNM
    X=A+0.5*DEL
    SUM=0.
    DO 200 J=1,IT
      SUM=SUM+FUNC(X)
      X=X+DEL
200  CONTINUE
    S=0.5*(S+(B-A)*SUM/TNM)
    IT=2*IT
  ENDIF
  RETURN
  END

```

```

SUBROUTINE QSIMPY(FUNC,A,B,S)
  PARAMETER (EPS=1.E-5, JMAX=20)
  OST=-1.E30
  OS= -1.E30
  DO 300 J=1,JMAX
    CALL TRAPZDY(FUNC,A,B,ST,J)
    S=(4.*ST-OST)/3.
    IF (ABS(S-OS).LT.EPS*ABS(OS)) RETURN
    OS=S
    OST=ST
300  CONTINUE

```

PAUSE 'Too many steps.'
END

Bibliography

1. Beran, Mark J. and Alan M. Whiteman. "Scintillation Index Calculations Using an Altitude-Dependent Structure Constant," *Applied Optics*, 27:2178-2181 (June 1988).
2. Fisher, M.J. and F.R. Krause. "The Crossed-Beam Correlation Method," *Journal of Fluid Mechanics*, 28:705-717 (June 1967).
3. Fried, David L. "Remote Sensing of the Optical Strength of Atmospheric Turbulence and Wind Velocity," *Proceedings of the IEEE*, 57:415-420 (October 1969).
4. Gardner, Chester S., et al. "Design and Performance Analysis of Adaptive Optical Telescopes Using Laser Guide Stars and Slope Sensors," *Proceedings of the IEEE*, 11:1721-1743 (November 1990).
5. Gaskill, Jack D. *Linear Systems, Fourier Transforms, and Optics*. New York: John Wiley and Sons, 1978.
6. Goodman, Joseph W. *Statistical Optics*. New York: John Wiley and Sons, 1985.
7. Hardy, J.W. "Active Optics: A New Technology for the Control of Light," *Proceedings of the IEEE*, 66:651-697 (June 1978).
8. Ishimaru, Akira. *Wave Propagation and Scattering in Random Media*, 2. New York: Academic Press, 1978.
9. Kolmogoroff, A. N. "The Local Structure of Turbulence in Incompressible Viscous Fluids for Very Large Reynolds Numbers." *Turbulence: Classic Papers on Statistical Theory* edited by Sheldon K. Friedlander and Leonard Topper, 151-155, New York: Interscience Publishers, 1961.
10. Kraus-Polstorff, J. and Donald Walters. "Refractive Turbulence Profiling Using an Orbiting Light Source," *Applied Optics*, 29:1877-1885 (May 1990).
11. Lutomirski, R.F. and R.G. Buser. "Mutual Coherence Function of a Finite Optical Beam and Application to Coherent Detection," *Applied Optics*, 12:2159-2160 (September 1973).
12. Ochs, G.R., et al. "Refractive Turbulence Profiles Measured by One-Dimensional Spatial Filtering of Scintillations," *Applied Optics*, 15:2504-2510 (October 1976).
13. Peskoff, Arthur. "Theory of Remote Sensing of Clear-Air Turbulence Profiles," *Journal of the Optical Society of America*, 58:1032-1040 (August 1968).
14. Rocca, A., et al. "Detection of Atmospheric Turbulent Layers by Spatiotemporal and Spatioangular Correlation Measurements of Stellar light Scintillations," *Journal of the Optical Society of America*, 61:1000-1004 (July 1974).
15. Tatarski, V.I. *Wave Propagation in a Turbulent Medium*. New York: McGraw-Hill Book Company, 1961. Translated from the Russian by R.A. Silverman.
16. Wallner, Edward P. "Optical Wave-Front Correction Using Slope Measurements," *Journal of the Optical Society of America*, 12:1771-1776 (December 1983).

17. Wang, Ting-i., et al. "Wind and Refractive Turbulence Sensing Using Crossed Laser Beams," *Applied Optics*, 13:2602-2608 (November 1974).
18. Welsh, Byron M. "Sensing Refractive Turbulence Profiles Using Wave Front Phase Measurements from Multiple Reference Sources," *SPIE Proceedings*, 1487:1-12 (April 1991).
19. Welsh, Byron M. and Chester S. Gardner. "Performance Analysis of Adaptive Optics Systems Using Laser Guide Stars and Slope Sensors," *Journal of the Optical Society of America*, 6:1913-1923 (December 1989).
20. Whalen, Anthony D. *Detection of Signals in Noise*. New York: Academic Press, 1971.

Vita

Michael D. Rejack was born in Schenectady, New York, on September 9, 1958. He enlisted in the United States Air Force in December 1977, and was selected for the Airman Education and Commissioning Program in 1982. He graduated cum laude with a Bachelor of Science degree in Electrical Engineering from the University of New Hampshire, Durham, New Hampshire, in December 1985. He was commissioned a second lieutenant in April 1986 and was promoted to the rank of captain while serving with the Air Force Space Command, Peterson AFB, Colorado, in April 1990. Captain Rejack entered the Air Force Institute of Technology in June, 1990. He is married to Cheryl Morency of Salem, Massachusetts. They have two children; Nicholas and Emily.

Permanent address: P.O. Box 1386
Hampton, New Hampshire
03842